

On optimal chamfer masks and coefficients

Grégoire Malandain — Céline Fouard

N° 5566

May 10, 2005

Thème BIO

 *apport
de recherche*

On optimal chamfer masks and coefficients

Grégoire Malandain , Céline Fouard

Thème BIO — Systèmes biologiques
Projet Epidaure

Rapport de recherche n° 5566 — May 10, 2005 — 36 pages

Abstract: This report describes the calculation of local errors in Chamfer masks both in two- and in three-dimensional anisotropic spaces. For these errors, closed forms are given that can be related to the Chamfer mask geometry. Thanks to these calculation, it can be observed that the usual Chamfer masks (*i.e.* $3 \times 3 \times 3$ or $5 \times 5 \times 5$) have an inhomogeneously distributed error. Moreover, it allows us to design dedicated Chamfer masks by controlling either the complexity of the computation of the distance map (or equivalently the number of vectors in the mask), or the error of the mask in \mathbb{Z}^2 or in \mathbb{Z}^3 . Last, since Chamfer distances are usually computed with integer weights (and approximate the Euclidean distance up to a multiplicative factor), we demonstrate that the knowledge of the local errors allows a very efficient computation of these weights.

Key-words: Chamfer distance, anisotropic lattice, Farey triangulation

Calcul de coefficients et de masques du chanfrein optimaux

Résumé : Ce rapport décrit le calcul d'erreurs locales dans des masques de distance du chanfrein en dimensions 2 et 3 dans des espaces anisotropes. Ces erreurs sont données par des formules analytiques simples qui peuvent être reliées à la géométrie du masque. Grâce à ces calculs, on peut se rendre compte que les masques usuels (*i.e.* 3x3x3 or 5x5x5) ont une erreur locale inhomogène. Cela nous permet de plus de construire des masques de distances du chanfrein dédiés, soit en contrôlant la complexité calculatoire de la carte de distance (plus exactement, le nombre de vecteurs du masque), ou l'erreur du masque dans \mathbb{Z}^2 ou \mathbb{Z}^3 . Finalement, comme les distances du chanfrein sont habituellement calculées avec des poids entiers (et approximent la distance euclidienne à une constante multiplicative près), nous montrons que la connaissance de ces erreurs locales permet un calcul très efficace de jeux de coefficients optimaux.

Mots-clés : Distance du chanfrein, grille anisotrope, triangulation de Farey

1 Introduction

Distance maps are a powerful tool for many image processing operations. Among others, they allow to perform mathematical morphology [1, 2] operations with large structuring elements, to guide skeletonization [3, 4], to interpolate [5, 6] or to morph images [7], to register images [8, 9], or to extract morphometric attributes from binary shapes [10].

Basically, a distance map is a grey-level image where the pixel or voxel value gives the distance towards a binary shape. A number of approaches have been proposed in the literature. Although some of them allow to compute the Euclidean Distance [11, 12, 13, 14, 15, 16, 17, 18, 19], the Chamfer Distance, that only yields an approximation of the Euclidean one, is still an appealing technique because of its advantages: a fast computation and an implementation simplicity even in extreme situation [20].

Chamfer distances have been introduced early in image processing [21, 22] and have been made popular by Borgefors [23, 24, 25]. It consists in approximating the path of any background point to the nearest foreground point by elementary displacements, given by the *Chamfer mask*, each of them being associated with an elementary cost, the *Chamfer coefficients*: the sum of the costs associated to the path gives a distance estimation from the background point to the nearest foreground point.

Given a Chamfer mask, the difficulty is then to estimate the associated *optimal* Chamfer coefficients, that are usually chosen integer for computational considerations. Optimality is achieved by minimizing the error with respect to the Euclidean distance. For isotropic cubic grids, in 2-D or in 3-D, these coefficients can be found in the literature. Their calculation for anisotropic grids have also been described [26, 27, 28]. This is important for biomedical applications (e.g. [29, 20]), where the 3-D acquisition devices (CT-scan, MRI, confocal microscope) usually provide a set of 2-D slices whose thickness is larger than the pixel size.

Since the anisotropy factor may vary from one acquisition to the next, it is mandatory to enable an on-line computation of the optimal Chamfer coefficients. This has been proposed in [30] for a relative error computed on a plane. However, the calculation of a set of optimal coefficients with large values, although automated, may still require a large computational time.

In this article, we provide the calculations of the optimal real Chamfer coefficients for an error calculated on a sphere, both in 2-D and in 3-D (sections 3 and 4). It not only yields simple closed forms but also a characterization of the sector where the maximal error occur. These results allow to design optimal Chamfer masks in \mathbb{Z}^2 and \mathbb{Z}^3 , and a much more efficient computation of optimal integer Chamfer coefficients for any Chamfer mask in any kind of 2-D or 3-D lattice.

2 Recalls

2.1 Definition and notations

Chamfer distances are usually defined (and used) in a discrete space or lattice denoted by \mathbb{S} : it may be chosen among the usual ones (e.g. $\mathbb{Z}^2, \mathbb{Z}^3$), or it can be more exotic (e.g. hexagonal grid).

Such discrete spaces are embedded into real spaces \mathbb{R}^2 or \mathbb{R}^3 , in which an orthogonal coordinates system can be defined by the frames $(O, \mathbf{x}, \mathbf{y})$ and $(O, \mathbf{x}, \mathbf{y}, \mathbf{z})$ respectively.

We also define a size factor along each of the frame axis, to introduce some space anisotropy. Typically, for $\mathbb{S} = \mathbb{Z}^2$, the couple (s_x, s_y) defines the pixel sizes in world units, while, for $\mathbb{S} = \mathbb{Z}^3$, the triplet (s_x, s_y, s_z) defines the voxel sizes.

In a discrete space \mathbb{S} , the chamfer distance is uniquely defined by its chamfer mask.

Definition 1 (Chamfer Mask) *A chamfer mask is a set of p couples $\mathcal{M} = \{(w_i, \mathbf{n}_i)\} \subset \mathbb{R}_+ \times \mathbb{S}$. that has some properties:*

- *it contains at least one basis of \mathbb{S}*
- *it is central-symmetric: $\forall (w_i, \mathbf{n}_i) \in \mathcal{M}, (w_i, -\mathbf{n}_i) \in \mathcal{M}$*
- *it has positive weights: $\forall (w_i, \mathbf{n}_i) \in \mathcal{M}, w_i > 0$ and $\mathbf{n}_i \neq \mathbf{0}$*
- *it only contains visible points [30].*

In the following, we will denote by \mathbf{v} the vector \mathbf{n} expressed in world units (*i.e.*, if $\mathbf{n} = (x, y)$, then $\mathbf{v} = (s_x x, s_y y)$), and by \mathbf{u} , the unit vector associated to \mathbf{v} , *i.e.* $\mathbf{u} = \mathbf{v} / \|\mathbf{v}\|$. The angle between two vectors \mathbf{v}_i and \mathbf{v}_j , or equivalently \mathbf{u}_i and \mathbf{u}_j , is denoted by θ_{ij} . We will also define the normalized weights ω_i by $\omega_i = w_i / \|\mathbf{v}_i\|$.

Since \mathcal{M} contains at least one basis of \mathbb{S} , for any two points P and Q of \mathbb{S} , we can build a path from P to Q as a linear combination (with integer weights) of the vectors \mathbf{n}_i . The set of paths from P to Q , denoted $\mathcal{P}(PQ)$ is defined by

$$\mathcal{P}(PQ) = \left\{ (a_i) \in \mathbb{N}^p \text{ such that } \overrightarrow{PQ} = \sum_i a_i \mathbf{n}_i \right\}$$

The cost of a path is now defined as the linear combination of the weights w_i , *i.e.* $\sum_i a_i w_i$.

Definition 2 (Chamfer distance) *The chamfer distance between P and Q , denoted $\tilde{D}(PQ)$ is the cost of the path of minimal cost from P to Q . Let*

$$(\hat{a}_i) = \arg \min_{(a_i) \in \mathcal{P}(PQ)} \sum_i a_i w_i \quad \text{then} \quad \tilde{D}(PQ) = \sum_i \hat{a}_i w_i$$

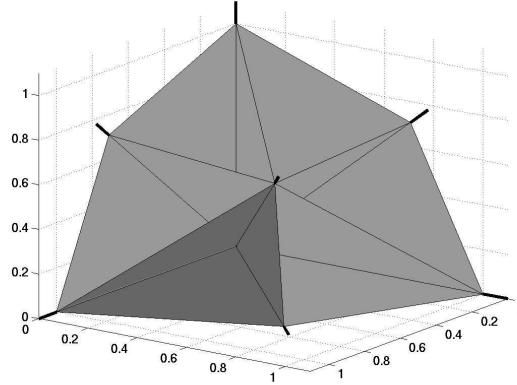


Figure 1: The 8 sectors of the 3x3x3 Chamfer mask in the first 1/8th of the space. Because of symmetries, only one of them (the darkest one) has to be considered in isotropic lattices.

2.2 Optimal coefficient calculation

The Chamfer distance is usually used as an approximation of the Euclidean one. The Chamfer coefficients have then to be chosen so as to minimize the error with respect to the Euclidean distance: it may be a relative or an absolute error, computed either on a plane or a sphere. We propose here to compute an absolute error on a sphere. For the error calculation, we will consider the chamfer distance from a point M to the coordinates origin O (since Chamfer distance are translation invariant [31]), that we denote by $\tilde{D}(M)$.

Generally, the calculation is reduced to the computation of *local* errors, which requires the decomposition of the Chamfer mask.

- In 2-D, it can be decomposed in doublets $(\mathbf{n}_i, \mathbf{n}_j)$ such that the angular sectors defined by those doublets do not overlap (we can not find a mask vector \mathbf{n}_l *between* \mathbf{n}_i and \mathbf{n}_j). The vectors in these doublets are ordered in direct order, hence the vectorial product $\mathbf{n}_i \times \mathbf{n}_j = x_i y_j - x_j y_i$ (considered as a scalar value in 2-D) is strictly positive. In 2-D, such a decomposition is straightforward.
- In 3-D, it can be decomposed in triplets $(\mathbf{n}_i, \mathbf{n}_j, \mathbf{n}_k)$ such that the (solid) angular sectors defined by those triplets do not overlap (we can not find a mask vector \mathbf{n}_l *between* \mathbf{n}_i , \mathbf{n}_j and \mathbf{n}_k): see figure 1. The vectors in these triplets are ordered in direct order, hence the scalar triple product $[\mathbf{n}_i, \mathbf{n}_j, \mathbf{n}_k]$ is strictly positive. In 3-D, such a decomposition is not unique: there exists several triangulations (or decompositions) of the same mask.

The computation is reduced to an error computation within each sector $(O, \mathbf{n}_i, \mathbf{n}_j, \mathbf{n}_k)$. Given a Chamfer mask decomposition, every point M can be expressed as an unique combination of the vectors \mathbf{n}_i

$$M = a\mathbf{n}_i + b\mathbf{n}_j + c\mathbf{n}_k \quad \text{with} \quad \{a, b, c\} \subset \mathbb{R}_+$$

the cone $(O, \mathbf{n}_i, \mathbf{n}_j, \mathbf{n}_k)$ being a sector that contains M (except for points on the sector borders, this sector is unique).

The local error computations are conducted in the real space (\mathbb{R}^2 or \mathbb{R}^3). They are valid in the discrete space \mathbb{S} , if the chamfer mask \mathcal{M} and its decomposition satisfy an additional assumption [32].

Assumption 1 (Chamfer mask) *For any doublet $(\mathbf{n}_i, \mathbf{n}_j)$ (resp. triplet $(\mathbf{n}_i, \mathbf{n}_j, \mathbf{n}_k)$), any point M of the discrete space \mathbb{S} lying in the sector $(O, \mathbf{n}_i, \mathbf{n}_j)$ (resp. $(O, \mathbf{n}_i, \mathbf{n}_j, \mathbf{n}_k)$), the vector \overrightarrow{OM} can be expressed as a linear combination of vectors \mathbf{n}_i and \mathbf{n}_j (resp. \mathbf{n}_i , \mathbf{n}_j , and \mathbf{n}_k) with positive integer coefficients.*

One has then to pay a great attention to the design of the Chamfer masks, especially in 3-D. For that reason, additional constraints on the Chamfer coefficients are introduced. For instance, Borgefors and colleagues usually use semi-regularity constraints [31].

In \mathbb{Z}^2 and \mathbb{Z}^3 , this assumption is also met if the Chamfer mask can be decomposed in *regular sectors* [22, 30]. Rémy and Thiel [33, 34, 35, 30] have shown that Farey sets are an adequate tool to build Chamfer masks made of *regular sectors* in \mathbb{Z}^2 and \mathbb{Z}^3 . In addition, they have shown that Chamfer distance may also induce norms, according that additional constraints, namely the *convexity constraints* (equations (17) and (19)), are verified.

In the following, we assume that the Chamfer mask used for the error computation satisfy all the above required properties for a local error computation.

3 Error calculation: the 2-D case

Let $M = (x, y)$, and $(\mathbf{n}_i, \mathbf{n}_j)$ be the sector that contains M . We have

$$M = a\mathbf{n}_i + b\mathbf{n}_j \quad \text{with} \quad a = \frac{1}{\mathbf{n}_i \times \mathbf{n}_j}(xy_j - x_jy) \quad \text{and} \quad b = \frac{1}{\mathbf{n}_i \times \mathbf{n}_j}(x_iy - xy_i) \quad (1)$$

The chamfer distance of M can be also expressed as a linear combination of its coordinates:

$$\tilde{D}(M) = aw_i + bw_j = \alpha x + \beta y$$

with

$$\alpha = \frac{1}{\mathbf{n}_i \times \mathbf{n}_j}(y_jw_i - y_iw_j) \quad \text{and} \quad \beta = \frac{1}{\mathbf{n}_i \times \mathbf{n}_j}(-x_jw_i + x_iw_j)$$

3.1 Calculation of the error extrema in a sector

Let us consider the absolute error between the chamfer distance and the Euclidean one (expressed in world units).

$$E(M) = \tilde{D}(M) - D(M) = \alpha x + \beta y - \sqrt{s_x^2 x^2 + s_y^2 y^2}$$

We will study this error on a circle of radius $R > 0$, and we restrict this study, without loss of generality to the first space quadrant ($x, y \geq 0$). On this circle, the error can be expressed as a function of y

$$E(M) = \alpha \frac{\sqrt{R^2 - s_y^2 y^2}}{s_x} + \beta y - R$$

We are looking for the error maximum, *i.e.* for $M_{ext} = \arg \max_M E(M)$. The derivative of the error function is

$$\frac{dE}{dy} = \beta - \alpha \frac{s_y^2}{s_x} \frac{y}{\sqrt{R^2 - s_y^2 y^2}}$$

that is zero for $y = y_{ext}$, with

$$y_{ext} = \frac{s_x}{s_y} \frac{\beta}{\sqrt{\beta^2 s_x^2 + \alpha^2 s_y^2}} R$$

The error $E(M)$ is then maximal at M_{ext} defined by

$$M_{ext} = (x_{ext}, y_{ext}) = \left(\frac{s_y}{s_x} \frac{\alpha}{\sqrt{\beta^2 s_x^2 + \alpha^2 s_y^2}} R, \frac{s_x}{s_y} \frac{\beta}{\sqrt{\beta^2 s_x^2 + \alpha^2 s_y^2}} R \right) \quad (2)$$

yielding the three possible error extrema in a sector

$$\begin{aligned} E(M_a) &= \omega_i R - R \\ E(M_b) &= \omega_j R - R \\ E(M_{ext}) &= \frac{\|\omega_i \mathbf{u}_j - \omega_j \mathbf{u}_i\|}{\mathbf{u}_i \times \mathbf{u}_j} R - R \end{aligned} \quad (3)$$

The calculation details can be found in section A.1.

In this computation, we do not pay attention whether the maximum M_{ext} is effectively reached, *i.e.* whether M_{ext} is effectively within the sector $(O, \mathbf{n}_i, \mathbf{n}_j)$.

Proposition 1 *The maximum M_{ext} of the error function $E(M)$ lies within the sector $(O, \mathbf{n}_i, \mathbf{n}_j)$ if and only if the two following conditions are verified.*

$$\frac{\|\mathbf{v}_j\|^2}{\mathbf{v}_i \cdot \mathbf{v}_j} \geq \frac{w_j}{w_i} \iff \frac{1}{\mathbf{u}_i \cdot \mathbf{u}_j} \geq \frac{\omega_j}{\omega_i} \quad (4a)$$

$$\frac{w_j}{w_i} \geq \frac{\mathbf{v}_i \cdot \mathbf{v}_j}{\|\mathbf{v}_i\|^2} \iff \frac{\omega_j}{\omega_i} \geq \mathbf{u}_i \cdot \mathbf{u}_j \quad (4b)$$

The calculation details can be found in section A.2.

If the conditions (4) are verified, the extrema of the error function on a circle of radius R are located at the three points M_a , M_b , and M_{ext} . M_a and M_b being respectively defined by $M_a = a\mathbf{n}_i$ and $M_b = b\mathbf{n}_j$ (see eq. (1)) while M_{ext} is defined in eq. (2).

This allows to determine both the maximum and minimum values of the error within a sector:

$$\text{if } \frac{1}{\mathbf{u}_i \cdot \mathbf{u}_j} \geq \frac{\omega_j}{\omega_i} \text{ and } \frac{\omega_j}{\omega_i} \geq \mathbf{u}_i \cdot \mathbf{u}_j \implies \begin{cases} E_{max} = \frac{\|\omega_i \mathbf{u}_j - \omega_j \mathbf{u}_i\|}{\mathbf{u}_i \times \mathbf{u}_j} R - R \\ E_{min} = \min(\omega_i R - R, \omega_j R - R) \end{cases} \quad (5a)$$

$$\text{if } \frac{1}{\mathbf{u}_i \cdot \mathbf{u}_j} \geq \frac{\omega_j}{\omega_i} \text{ and } \frac{\omega_j}{\omega_i} < \mathbf{u}_i \cdot \mathbf{u}_j \implies \begin{cases} E_{max} = \omega_i R - R \\ E_{min} = \omega_j R - R \end{cases} \quad (5b)$$

$$\text{if } \frac{1}{\mathbf{u}_i \cdot \mathbf{u}_j} < \frac{\omega_j}{\omega_i} \text{ and } \frac{\omega_j}{\omega_i} \geq \mathbf{u}_i \cdot \mathbf{u}_j \implies \begin{cases} E_{max} = \omega_j R - R \\ E_{min} = \omega_i R - R \end{cases} \quad (5c)$$

3.2 The best possible error in a 2-D sector

Since the pioneering publications of Borgefors [23, 24, 25] that have popularized the chamfer distance, minimizing the error within a sector $(O, \mathbf{n}_i, \mathbf{n}_j)$ is a well known procedure. It comes to set the same error (in absolute value) at the three extrema, two of them, $E(M_a)$ and $E(M_b)$, being negative while the last one, $E(M_{ext})$, is positive. We then have to solve the following equalities

$$-E(M_a) = -E(M_b) = E(M_{ext})$$

From $E(M_a) = E(M_b)$, it comes that $\omega_i = \omega_j$. By substituting ω_j by ω_i in $E(M_{ext}) = -E(M_a)$, it comes

$$\omega_i = \omega_j = \omega_{opt} = \frac{2}{\frac{\|\mathbf{u}_j - \mathbf{u}_i\|}{\mathbf{u}_i \times \mathbf{u}_j} + 1} = \frac{2H_{ij}}{1 + H_{ij}} \quad \text{with} \quad H_{ij} = \frac{\mathbf{u}_i \times \mathbf{u}_j}{\|\mathbf{u}_j - \mathbf{u}_i\|} = \frac{\|\mathbf{u}_i + \mathbf{u}_j\|}{2} \quad (6)$$

H_{ij} being the height of the triangle OU_iU_j that is associated to the sector $(O, \mathbf{u}_i, \mathbf{u}_j)$, by $U_i = O + \mathbf{u}_i$ and $U_j = O + \mathbf{u}_j$ (see figure 2). Since the \mathbf{u} 's are unit vectors, $(\mathbf{u}_i + \mathbf{u}_j)$ is orthogonal to $(\mathbf{u}_j - \mathbf{u}_i)$, it comes then that

$$\|\mathbf{u}_j - \mathbf{u}_i\| = \left\| (\mathbf{u}_j - \mathbf{u}_i) \times \frac{\mathbf{u}_i + \mathbf{u}_j}{\|\mathbf{u}_i + \mathbf{u}_j\|} \right\|$$

By developing, we get $\|(\mathbf{u}_j - \mathbf{u}_i) \times (\mathbf{u}_i + \mathbf{u}_j)\| = 2\|\mathbf{u}_i \times \mathbf{u}_j\|$ hence $\frac{\mathbf{u}_i \times \mathbf{u}_j}{\|\mathbf{u}_j - \mathbf{u}_i\|} = \frac{\|\mathbf{u}_i + \mathbf{u}_j\|}{2}$.

It has to be pointed out that, by choosing $\omega_i = \omega_j$, the conditions (4) are always verified (the maximum M_{ext} lies within the sector $(O, \mathbf{n}_i, \mathbf{n}_j)$). We obtain then the value E_{opt} of the best possible error within this sector $(O, \mathbf{n}_i, \mathbf{n}_j)$

$$E_{opt} = \frac{\frac{\|\mathbf{u}_j - \mathbf{u}_i\|}{\mathbf{u}_i \times \mathbf{u}_j} - 1}{\frac{\|\mathbf{u}_j - \mathbf{u}_i\|}{\mathbf{u}_i \times \mathbf{u}_j} + 1} R = \frac{1 - H_{ij}}{1 + H_{ij}} R \quad (7)$$

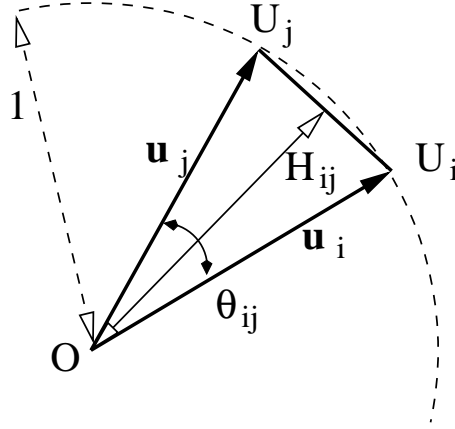


Figure 2: Notations for proposition 2.

Proposition 2 *The triangle OU_iU_j that has the smallest height (associated to the edge opposed to O) is associated to the sector $(O, \mathbf{u}_i, \mathbf{u}_j)$ of maximal best possible error.*

This is straightforward since the best possible error is given by equation (7), and since $H_{ij} = \frac{\|\mathbf{u}_i + \mathbf{u}_j\|}{2}$ is the height (associated to the edge opposed to O) of the triangle OU_iU_j .

Proposition 3 *The sector $(O, \mathbf{u}_i, \mathbf{u}_j)$ with the largest angle θ_{ij} between the vectors \mathbf{u}_i and \mathbf{u}_j is the one of maximal best possible error.*

This is straightforward since $\|\mathbf{u}_i + \mathbf{u}_j\| = 2 \cos \frac{\theta_{ij}}{2}$, and then $H_{ij} = \cos \frac{\theta_{ij}}{2}$. We can also express the above minimum error by

$$E(M_{ext}) = \frac{1 - \cos \frac{\theta_{ij}}{2}}{1 + \cos \frac{\theta_{ij}}{2}} R \quad (8)$$

3.3 The best possible error of a mask

Proposition 4 *The best possible error of a chamfer mask \mathcal{M} is the maximum of the best possible errors of all sectors $(O, \mathbf{u}_i, \mathbf{u}_j)$, i.e.*

$$E_{opt}(\{\mathbf{n}_1, \dots, \mathbf{n}_p\}) = \max_{(O, \mathbf{u}_k, \mathbf{u}_l)} E_{opt}(O, \mathbf{u}_k, \mathbf{u}_l)$$

Let $(O, \mathbf{u}_i, \mathbf{u}_j)$ be the sector that yield the maximum of the best possible errors over all sectors, i.e. $H_{ij} \leq H_{kl}, \forall$ sector $(O, \mathbf{u}_k, \mathbf{u}_l)$ and let $\omega_{opt} = \frac{2H_{ij}}{1+H_{ij}}$ (see eq. (6)).

Let us make equal all the normalized weights ω_k , *i.e.* $\omega_k = \omega_{opt}, \forall k$. It can easily be verified that eq. (4) are verified for every sector $(O, \mathbf{u}_k, \mathbf{u}_l)$.

The minimum error over the chamfer mask is then

$$E_{min}(\{\mathbf{n}_1, \dots, \mathbf{n}_p\}) = \min_k \omega_k R - R = \omega_{opt} R - R = E_{opt}(O, \mathbf{u}_i, \mathbf{u}_j) \quad \text{since } \omega_k = \omega_{opt}, \forall k$$

The maximum error over the chamfer mask is then (case (5a))

$$\begin{aligned} E_{max}(\{\mathbf{n}_1, \dots, \mathbf{n}_p\}) &= \max_{(O, \mathbf{u}_k, \mathbf{u}_l)} \frac{\|\omega_k \mathbf{u}_l - \omega_l \mathbf{u}_k\|}{\mathbf{u}_k \times \mathbf{u}_l} R - R \\ &= \max_{(O, \mathbf{u}_k, \mathbf{u}_l)} \frac{\omega_{opt}}{H_{kl}} R - R = \frac{\omega_{opt}}{H_{ij}} R - R = E_{opt}(O, \mathbf{u}_i, \mathbf{u}_j) \end{aligned}$$

We have then exhibit a set of normalized weights so that the error of the chamfer mask is the best possible error of the sector of minimal height. Let us remark that, in the general case, this set is not unique and there may exist other weight sets in \mathbb{R}^p that yield the same error.

Moreover, the best possible error of a chamfer mask is given by

$$E_{opt}(\{\mathbf{n}_1, \dots, \mathbf{n}_p\}) = \frac{1 - H_{ij}}{1 + H_{ij}} R \quad \text{with } H_{ij} = \min_{(O, \mathbf{u}_k, \mathbf{u}_l)} H_{kl} \quad (9)$$

4 Error calculation: the 3-D case

Let $M = (x, y, z)$, and $(\mathbf{n}_i, \mathbf{n}_j, \mathbf{n}_k)$ be the sector that contains M . We have

$$M = a\mathbf{n}_i + b\mathbf{n}_j + c\mathbf{n}_k \quad \text{with} \quad \begin{cases} a = \frac{(y_j z_k - y_k z_j)x + (x_k z_j - x_j z_k)y + (x_j y_k - x_k y_j)z}{x_i y_j z_k + x_j y_k z_i + x_k y_i z_j - x_i y_k z_j - x_j y_i z_k - x_k y_j z_i} \\ b = \frac{(y_k z_i - y_i z_k)x + (x_i z_k - x_k z_i)y + (x_k y_i - x_i y_k)z}{x_i y_j z_k + x_j y_k z_i + x_k y_i z_j - x_i y_k z_j - x_j y_i z_k - x_k y_j z_i} \\ c = \frac{(y_i z_j - y_j z_i)x + (x_j z_i - x_i z_j)y + (x_i y_j - x_j y_i)z}{x_i y_j z_k + x_j y_k z_i + x_k y_i z_j - x_i y_k z_j - x_j y_i z_k - x_k y_j z_i} \end{cases} \quad (10)$$

or

$$a = \frac{(\mathbf{n}_j \times \mathbf{n}_k) \cdot M}{[\mathbf{n}_i, \mathbf{n}_j, \mathbf{n}_k]} \quad \text{and} \quad b = \frac{(\mathbf{n}_k \times \mathbf{n}_i) \cdot M}{[\mathbf{n}_i, \mathbf{n}_j, \mathbf{n}_k]} \quad \text{and} \quad c = \frac{(\mathbf{n}_i \times \mathbf{n}_j) \cdot M}{[\mathbf{n}_i, \mathbf{n}_j, \mathbf{n}_k]} \quad (11)$$

The chamfer distance of M can be also expressed as a linear combination of its coordinates:

$$\tilde{D}(M) = aw_i + bw_j + cw_k = \alpha x + \beta y + \gamma z$$

with

$$\begin{cases} \alpha = \frac{1}{[\mathbf{n}_i, \mathbf{n}_j, \mathbf{n}_k]} ((y_j z_k - y_k z_j)w_i + (y_k z_i - y_i z_k)w_j + (y_i z_j - y_j z_i)w_k) \\ \beta = \frac{1}{[\mathbf{n}_i, \mathbf{n}_j, \mathbf{n}_k]} ((x_k z_j - x_j z_k)w_i + (x_i z_k - x_k z_i)w_j + (x_j z_i - x_i z_j)w_k) \\ \gamma = \frac{1}{[\mathbf{n}_i, \mathbf{n}_j, \mathbf{n}_k]} ((x_j y_k - x_k y_j)w_i + (x_k y_i - x_i y_k)w_j + (x_i y_j - x_j y_i)w_k) \end{cases} \quad (12)$$

or

$$\begin{pmatrix} \alpha \\ \beta \\ \gamma \end{pmatrix} = \frac{1}{[\mathbf{n}_i, \mathbf{n}_j, \mathbf{n}_k]} ((\mathbf{n}_j \times \mathbf{n}_k)w_i + (\mathbf{n}_k \times \mathbf{n}_i)w_j + (\mathbf{n}_i \times \mathbf{n}_j)w_k) \quad (13)$$

4.1 Calculation of the error extrema in a sector

Let us consider the absolute error between the chamfer distance and the Euclidean one (expressed in world units).

$$E(M) = \tilde{D}(M) - D(M) = \alpha x + \beta y + \gamma z - \sqrt{s_x^2 x^2 + s_y^2 y^2 + s_z^2 z^2}$$

We will study this error on a sphere of radius $R > 0$, and we restrict this study, without loss of generality to the first space quadrant ($x, y, z \geq 0$). On this sphere, the error can be expressed as a function of y and z

$$E(M) = \alpha \sqrt{(R^2 - s_y^2 y^2 - s_z^2 z^2)/s_x^2} + \beta y + \gamma z - R$$

We are looking for the error maximum, *i.e.* for $M_{ext} = \arg \max_M E(M)$. The derivatives of the error function are

$$\frac{dE}{dy} = \beta - \alpha \frac{s_y^2}{s_x} \frac{y}{\sqrt{R^2 - s_y^2 y^2 - s_z^2 z^2}} \quad \text{and} \quad \frac{dE}{dz} = \gamma - \alpha \frac{s_z^2}{s_x} \frac{z}{\sqrt{R^2 - s_y^2 y^2 - s_z^2 z^2}}$$

$\frac{dE}{dy} = 0$ yields $s_y^2 y^2 = \beta^2 s_x^2 \frac{R^2 - s_z^2 z^2}{\alpha^2 s_y^2 + \beta^2 s_x^2}$. Reporting this expression into $\frac{dE}{dz} = 0$ gives

$$z_{ext} = \frac{s_x s_y}{s_z} \frac{\gamma}{\sqrt{\alpha^2 s_y^2 s_z^2 + \beta^2 s_x^2 s_z^2 + \gamma^2 s_x^2 s_y^2}} R$$

Finally, we obtain that the error $E(M)$ is then maximal at M_{ext} defined by

$$M_{ext} = \begin{pmatrix} x_{ext} \\ y_{ext} \\ z_{ext} \end{pmatrix} = \begin{pmatrix} \frac{s_y s_z}{s_x} \frac{\alpha}{\sqrt{\alpha^2 s_y^2 s_z^2 + \beta^2 s_x^2 s_z^2 + \gamma^2 s_x^2 s_y^2}} R \\ \frac{s_x s_z}{s_y} \frac{\beta}{\sqrt{\alpha^2 s_y^2 s_z^2 + \beta^2 s_x^2 s_z^2 + \gamma^2 s_x^2 s_y^2}} R \\ \frac{s_x s_y}{s_z} \frac{\gamma}{\sqrt{\alpha^2 s_y^2 s_z^2 + \beta^2 s_x^2 s_z^2 + \gamma^2 s_x^2 s_y^2}} R \end{pmatrix} \quad (14)$$

yielding

$$\begin{aligned}
E(M_a) &= \omega_i R - R \\
E(M_b) &= \omega_j R - R \\
E(M_c) &= \omega_k R - R \\
E(M_{ext}) &= \frac{\|\omega_i(\mathbf{u}_j \times \mathbf{u}_k) + \omega_j(\mathbf{u}_k \times \mathbf{u}_i) + \omega_k(\mathbf{u}_i \times \mathbf{u}_j)\|}{[\mathbf{u}_i, \mathbf{u}_j, \mathbf{u}_k]} R - R
\end{aligned}$$

The calculation details can be found in section B.1.

In this computation, we do not pay attention whether this maximum is effectively reached, *i.e.* whether M_{ext} is effectively within the sector $(O, \mathbf{n}_i, \mathbf{n}_j, \mathbf{n}_k)$.

Proposition 5 *The maximum M_{ext} of the error function $E(M)$ lies within the sector $(O, \mathbf{n}_i, \mathbf{n}_j, \mathbf{n}_k)$ if and only if the three following conditions are verified.*

$$(\omega_i(\mathbf{u}_j \times \mathbf{u}_k) + \omega_j(\mathbf{u}_k \times \mathbf{u}_i) + \omega_k(\mathbf{u}_i \times \mathbf{u}_j)) \cdot (\mathbf{u}_j \times \mathbf{u}_k) \geq 0 \quad (15a)$$

$$(\omega_i(\mathbf{u}_j \times \mathbf{u}_k) + \omega_j(\mathbf{u}_k \times \mathbf{u}_i) + \omega_k(\mathbf{u}_i \times \mathbf{u}_j)) \cdot (\mathbf{u}_k \times \mathbf{u}_i) \geq 0 \quad (15b)$$

$$(\omega_i(\mathbf{u}_j \times \mathbf{u}_k) + \omega_j(\mathbf{u}_k \times \mathbf{u}_i) + \omega_k(\mathbf{u}_i \times \mathbf{u}_j)) \cdot (\mathbf{u}_i \times \mathbf{u}_j) \geq 0 \quad (15c)$$

The calculation details can be found in section B.2.

If the conditions (15) are verified, the extrema of the error function on a sphere of radius R are located at the three points M_a , M_b , M_c , and M_{ext} . M_a , M_b and M_c being respectively defined by $M_a = a\mathbf{n}_i$, $M_b = b\mathbf{n}_j$ and $M_c = c\mathbf{n}_k$ (see eq. (10)) while M_{ext} is defined in eq. (14).

This allows to determine both the maximum and minimum values of the error within a sector. Depending of the number of positive inequalities in eq. (15), there are three types of relative position of vector $U_{ijk} = \omega_i(\mathbf{u}_j \times \mathbf{u}_k) + \omega_j(\mathbf{u}_k \times \mathbf{u}_i) + \omega_k(\mathbf{u}_i \times \mathbf{u}_j)$ with respect to the sector $(O, \mathbf{n}_i, \mathbf{n}_j, \mathbf{n}_k)$ (see figure 3).

1. The three scalar products are positive. The maximum of error, E_{max} is reached at M_{ext} (figure 3(a)).
2. Two scalar products are positive. The maximum of error is reached along an edge. Figure 3(b) depicts the case where $U_{ijk} \cdot (\mathbf{u}_j \times \mathbf{u}_k) < 0$: the maximum of error is then reached within the 2-D sector $(O, \mathbf{u}_j, \mathbf{u}_k)$ and is equal to $E_{max} = \frac{\|\omega_j \mathbf{u}_k - \omega_k \mathbf{u}_j\|}{\|\mathbf{u}_j \times \mathbf{u}_k\|} R - R$ (cf eq. (3)).
3. Only one scalar product is positive. The maximum of error is reached at a vertex. Figure 3(c) depicts the case where $U_{ijk} \cdot (\mathbf{u}_j \times \mathbf{u}_k) < 0$ and $U_{ijk} \cdot (\mathbf{u}_k \times \mathbf{u}_i) < 0$: the maximum of error is then reached along vector \mathbf{u}_i and is equal to $E_{max} = \omega_i R - R$.

In the three cases, one may consider that the minimum of error is $E_{min} = \min(\omega_i R - R, \omega_j R - R, \omega_k R - R)$.

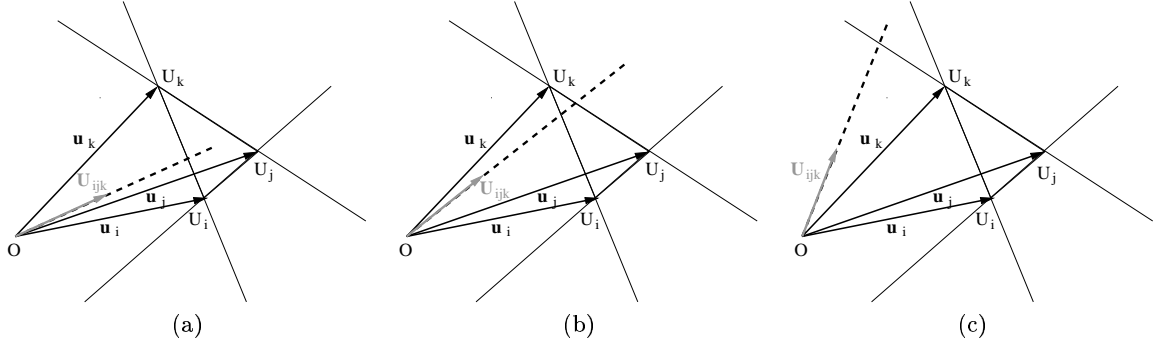


Figure 3: The different possible configuration with respect to the number of positive inequalities. (a) the 3 inequalities are positive; (b) two of them are positive; (c) only one of them is positive.

4.2 The best possible error in a 3-D sector

To minimize the maximal absolute error in a sector $(O, \mathbf{n}_i, \mathbf{n}_j, \mathbf{n}_k)$, we have to solve the following equalities

$$-E(M_a) = -E(M_b) = -E(M_c) = E(M_{ext})$$

From $E(M_a) = E(M_b) = E(M_c)$, it comes that $\omega_i = \omega_j = \omega_k$. By substituting both ω_j and ω_k by ω_i in $E(M_{ext}) = -E(M_a)$, it comes

$$\omega_i = \omega_j = \omega_k = \frac{2}{\frac{\|(\mathbf{u}_j \times \mathbf{u}_k) + (\mathbf{u}_k \times \mathbf{u}_i) + (\mathbf{u}_i \times \mathbf{u}_j)\|}{[\mathbf{u}_i, \mathbf{u}_j, \mathbf{u}_k]} + 1} = \frac{2H_{ijk}}{1 + H_{ijk}}$$

with

$$H_{ijk} = \frac{[\mathbf{u}_i, \mathbf{u}_j, \mathbf{u}_k]}{\|(\mathbf{u}_j \times \mathbf{u}_k) + (\mathbf{u}_k \times \mathbf{u}_i) + (\mathbf{u}_i \times \mathbf{u}_j)\|}$$

and we obtain then

$$E(M_{ext}) = \frac{\frac{\|(\mathbf{u}_j \times \mathbf{u}_k) + (\mathbf{u}_k \times \mathbf{u}_i) + (\mathbf{u}_i \times \mathbf{u}_j)\|}{[\mathbf{u}_i, \mathbf{u}_j, \mathbf{u}_k]} - 1}{\frac{\|(\mathbf{u}_j \times \mathbf{u}_k) + (\mathbf{u}_k \times \mathbf{u}_i) + (\mathbf{u}_i \times \mathbf{u}_j)\|}{[\mathbf{u}_i, \mathbf{u}_j, \mathbf{u}_k]} + 1} R = \frac{1 - H_{ijk}}{1 + H_{ijk}} R \quad (16)$$

Let us demonstrate that H_{ijk} is the height of the tetrahedron $OU_iU_jU_k$, built from the sector $(O, \mathbf{u}_i, \mathbf{u}_j, \mathbf{u}_k)$ with $U_i = O + \mathbf{u}_i$, $U_j = O + \mathbf{u}_j$, and $U_k = O + \mathbf{u}_k$ (see figure 3).

First, it can be noticed that the vector $\mathbf{U}_{ijk} = (\mathbf{u}_j \times \mathbf{u}_k) + (\mathbf{u}_k \times \mathbf{u}_i) + (\mathbf{u}_i \times \mathbf{u}_j)$ is orthogonal to the plane that contains the points U_i , U_j , and U_k : indeed the scalar vector of \mathbf{U}_{ijk} with each of the three vectors $\mathbf{u}_j - \mathbf{u}_i$, $\mathbf{u}_k - \mathbf{u}_j$, and $\mathbf{u}_i - \mathbf{u}_k$ is zero.

We can then write the equation of this plane as $\mathbf{U}_{ijk} \cdot \mathbf{M} - \mathbf{U}_{ijk} \cdot \mathbf{u}_i = 0$. The last term $\mathbf{U}_{ijk} \cdot \mathbf{u}_i$ being equal to $[\mathbf{u}_i, \mathbf{u}_j, \mathbf{u}_k]$, it comes out that this plane equation is then

$\mathbf{U}_{ijk}M - [\mathbf{u}_i, \mathbf{u}_j, \mathbf{u}_k] = 0$. The distance of any point to this plane can be computed by $\frac{|\mathbf{U}_{ijk}M - [\mathbf{u}_i, \mathbf{u}_j, \mathbf{u}_k]|}{\|\mathbf{U}_{ijk}\|}$. It comes out that $\frac{[\mathbf{u}_i, \mathbf{u}_j, \mathbf{u}_k]}{\|\mathbf{U}_{ijk}\|}$ is nothing but the distance of O to the plane $U_iU_jU_k$, i.e. the height of the tetrahedron.

However, unlike the 2-D case, setting $\omega_i = \omega_j = \omega_k$ does not ensure that the conditions (15) are verified. In this particular case, these conditions depend on the sign of the three scalar products of vector \mathbf{U}_{ijk} with vectors $(\mathbf{u}_j \times \mathbf{u}_k)$, $(\mathbf{u}_k \times \mathbf{u}_i)$, and $(\mathbf{u}_i \times \mathbf{u}_j)$. There are only two possible cases.

1. The three scalar products are positive. The height is effectively within the sector $(O, \mathbf{n}_i, \mathbf{n}_j, \mathbf{n}_k)$ and the theoretical minimal error of the sector is given by equation (16). This case is depicted by figure 3(a).
2. Two scalar products are positive, while the third is strictly negative. The height is located on the other side of an edge. Let us consider the case $\mathbf{U}_{ijk} \cdot (\mathbf{u}_j \times \mathbf{u}_k) < 0$ depicted by figure 3(b). The error will then be maximal along U_jU_k . The best possible error is then given by the 2-D formula (7) applied to the 2-D sector $(O, \mathbf{u}_j, \mathbf{u}_k)$, i.e.

$$\omega_j = \omega_k = \omega_{opt} = \frac{2H_{jk}}{1 + H_{jk}} \quad \text{and} \quad E_{opt} = \frac{1 - H_{jk}}{1 + H_{jk}} R$$

It can be shown that $\mathbf{U}_{ijk} \cdot (\mathbf{u}_j \times \mathbf{u}_k) < 0$ implies both $H_{jk} < H_{ij}$ and $H_{jk} < H_{ki}$ (see section B.3): this imply that the errors inside the 2-D sectors $(O, \mathbf{u}_i, \mathbf{u}_j)$ and $(O, \mathbf{u}_k, \mathbf{u}_i)$ and the 3-D sector $(O, \mathbf{u}_i, \mathbf{u}_j, \mathbf{u}_k)$ are strictly inferior to E_{opt} . As a consequence, this allows a certain freedom in the choice of ω_i .

3. Having two strictly negative scalar products (the case depicted in figure 3(c)) is not possible. Indeed, if one assumes that $\mathbf{U}_{ijk} \cdot (\mathbf{u}_j \times \mathbf{u}_k) < 0$ and $\mathbf{U}_{ijk} \cdot (\mathbf{u}_k \times \mathbf{u}_i) < 0$, it implies both $H_{jk} < H_{ki}$ (from the first inequality) and $H_{ki} < H_{jk}$ (from the second one) which is contradictory.

Proposition 6 *The tetrahedron $OU_iU_jU_k$ that has the smallest H , with*

$$H = \begin{cases} H_{ijk} & \text{if } \mathbf{U}_{ijk} \cdot (\mathbf{u}_j \times \mathbf{u}_k) \geq 0, \quad \mathbf{U}_{ijk} \cdot (\mathbf{u}_k \times \mathbf{u}_i) \geq 0, \quad \text{and} \quad \mathbf{U}_{ijk} \cdot (\mathbf{u}_i \times \mathbf{u}_j) \geq 0 \\ H_{jk} & \text{if } \mathbf{U}_{ijk} \cdot (\mathbf{u}_j \times \mathbf{u}_k) < 0, \quad \mathbf{U}_{ijk} \cdot (\mathbf{u}_k \times \mathbf{u}_i) \geq 0, \quad \text{and} \quad \mathbf{U}_{ijk} \cdot (\mathbf{u}_i \times \mathbf{u}_j) \geq 0 \\ H_{ik} & \text{if } \mathbf{U}_{ijk} \cdot (\mathbf{u}_j \times \mathbf{u}_k) \geq 0, \quad \mathbf{U}_{ijk} \cdot (\mathbf{u}_k \times \mathbf{u}_i) < 0, \quad \text{and} \quad \mathbf{U}_{ijk} \cdot (\mathbf{u}_i \times \mathbf{u}_j) \geq 0 \\ H_{ij} & \text{if } \mathbf{U}_{ijk} \cdot (\mathbf{u}_j \times \mathbf{u}_k) \geq 0, \quad \mathbf{U}_{ijk} \cdot (\mathbf{u}_k \times \mathbf{u}_i) \geq 0, \quad \text{and} \quad \mathbf{U}_{ijk} \cdot (\mathbf{u}_i \times \mathbf{u}_j) < 0 \end{cases}$$

is associated to the sector $(O, \mathbf{u}_i, \mathbf{u}_j, \mathbf{u}_k)$ of maximal minimum error.

4.3 The best possible error of a mask

Proposition 7 *The best possible error of a chamfer mask \mathcal{M} is the maximum of the best possible errors of all sectors $(O, \mathbf{u}_i, \mathbf{u}_j, \mathbf{u}_k)$, i.e.*

$$E_{opt}(\{\mathbf{n}_1, \dots, \mathbf{n}_p\}) = \max_{(O, \mathbf{u}_l, \mathbf{u}_m, \mathbf{u}_n)} E_{opt}(O, \mathbf{u}_l, \mathbf{u}_m, \mathbf{u}_n)$$

The proof is strictly similar to the one of the 2-D case.

As in 2-D, we can exhibit a weight set in \mathbb{R}^p that realize this error, and this set is not unique in the general case.

5 Convexity criteria

Convexity criteria have been introduced by [33]. They allow to ensure that a chamfer distance is also a norm. Surprisingly, one can demonstrate that the conditions of existence of the maximum M_{ext} within a sector (eq. (4) and (15)) do imply the convexity criterium. Unfortunately, since the equivalence is false (counter-examples can be exhibited), this is useless in practice (for the calculation of optimal integer weights, see below).

5.1 The 2-D case

Proposition 8 *The conditions (4) imply the convexity of the chamfer mask.*

The 2D convexity criterium has to be evaluated on two adjacent sectors $(O, \mathbf{u}_i, \mathbf{u}_j)$ and $(O, \mathbf{u}_j, \mathbf{u}_k)$ and is defined by

$$C_{ijk} = \begin{vmatrix} x_i & x_j & x_k \\ y_i & y_j & y_k \\ w_i & w_j & w_k \end{vmatrix} \geq 0 \quad (17)$$

it expresses the fact that the triangle defined by the extremities of the vectors \mathbf{v}_n/w_n (the above expression have to be multiplied by $s_x s_y$) must have a positive area. This criterium can be rewritten into

$$w_k(x_i y_j - x_j y_i) + w_j(x_k y_i - x_i y_k) + w_i(x_j y_k - x_k y_j) \geq 0$$

The conditions (4) for the sector $(O, \mathbf{u}_j, \mathbf{u}_k)$ are

$$\frac{\|\mathbf{v}_k\|^2}{\mathbf{v}_j \cdot \mathbf{v}_k} \geq \frac{w_k}{w_j} \iff \frac{1}{\mathbf{u}_j \cdot \mathbf{u}_k} \geq \frac{\omega_k}{\omega_j} \quad (18a)$$

$$\frac{w_k}{w_j} \geq \frac{\mathbf{v}_j \cdot \mathbf{v}_k}{\|\mathbf{v}_j\|^2} \iff \frac{\omega_k}{\omega_j} \geq \mathbf{u}_j \cdot \mathbf{u}_k \quad (18b)$$

From inequalities (4a) and (18b), it comes

$$\begin{aligned} & w_k(x_i y_j - x_j y_i) + w_j(x_k y_i - x_i y_k) + w_i(x_j y_k - x_k y_j) \\ & \geq \frac{w_j}{\|\mathbf{v}_j\|^2} ((\mathbf{v}_j \cdot \mathbf{v}_k)(x_i y_j - x_j y_i) + \|\mathbf{v}_j\|^2(x_k y_i - x_i y_k) + (\mathbf{v}_i \cdot \mathbf{v}_j)(x_j y_k - x_k y_j)) \end{aligned}$$

After developing the last term, it comes out that it is equal to zero, which proves proposition 8.

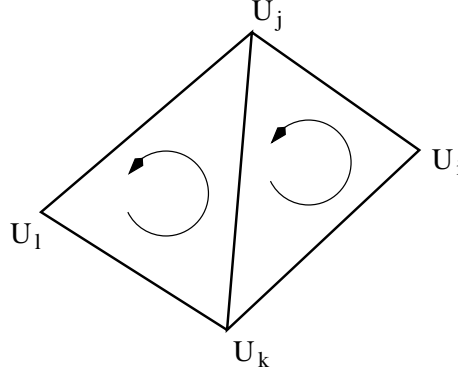


Figure 4: Notations for proposition 9.

5.2 The 3-D case

Proposition 9 *The conditions (15) imply the convexity of the chamfer mask.*

The 3D convexity criterium has to be evaluated on two adjacent sectors $(O, \mathbf{u}_i, \mathbf{u}_j, \mathbf{u}_k)$ and $(O, \mathbf{u}_j, \mathbf{u}_l, \mathbf{u}_k)$ (so we have $[\mathbf{u}_j, \mathbf{u}_l, \mathbf{u}_k] \geq 0$, see figure 4) and is defined by

$$C_{ijkl} = \begin{vmatrix} x_i & x_j & x_k & x_l \\ y_i & y_j & y_k & y_l \\ z_i & z_j & z_k & z_l \\ w_i & w_j & w_k & w_l \end{vmatrix} \geq 0 \quad (19)$$

it expresses the fact that the tetrahedra defined by the extremities of the vectors \mathbf{v}_n/w_n (the above expression has to be multiplied by $s_x s_y s_z$) must have a positive area. This criterium can be rewritten into

$$C_{ijkl} = w_l[\mathbf{n}_i, \mathbf{n}_j, \mathbf{n}_k] - w_k[\mathbf{n}_i, \mathbf{n}_j, \mathbf{n}_l] + w_j[\mathbf{n}_i, \mathbf{n}_k, \mathbf{n}_l] - w_i[\mathbf{n}_j, \mathbf{n}_k, \mathbf{n}_l]$$

After multiplication by $s_x s_y s_z$ and division by $\|\mathbf{v}_i\| \|\mathbf{v}_j\| \|\mathbf{v}_k\| \|\mathbf{v}_l\|$, we get

$$\begin{aligned} C_{ijkl} &\geq 0 \\ \iff \omega_l[\mathbf{u}_i, \mathbf{u}_j, \mathbf{u}_k] - \omega_k[\mathbf{u}_i, \mathbf{u}_j, \mathbf{u}_l] + \omega_j[\mathbf{u}_i, \mathbf{u}_k, \mathbf{u}_l] - \omega_i[\mathbf{u}_j, \mathbf{u}_k, \mathbf{u}_l] &\geq 0 \\ \iff \omega_l[\mathbf{u}_i, \mathbf{u}_j, \mathbf{u}_k] - \omega_k[\mathbf{u}_i, \mathbf{u}_j, \mathbf{u}_l] + \omega_j[\mathbf{u}_i, \mathbf{u}_k, \mathbf{u}_l] + \omega_i[\mathbf{u}_j, \mathbf{u}_l, \mathbf{u}_k] &\geq 0 \end{aligned}$$

The conditions (15) for the sector $(O, \mathbf{u}_j, \mathbf{u}_l, \mathbf{u}_k)$ are

$$(\omega_j(\mathbf{u}_l \times \mathbf{u}_k) + \omega_l(\mathbf{u}_k \times \mathbf{u}_j) + \omega_k(\mathbf{u}_j \times \mathbf{u}_l)) \cdot (\mathbf{u}_l \times \mathbf{u}_k) \geq 0 \quad (20a)$$

$$(\omega_j(\mathbf{u}_l \times \mathbf{u}_k) + \omega_l(\mathbf{u}_k \times \mathbf{u}_j) + \omega_k(\mathbf{u}_j \times \mathbf{u}_l)) \cdot (\mathbf{u}_k \times \mathbf{u}_j) \geq 0 \quad (20b)$$

$$(\omega_j(\mathbf{u}_l \times \mathbf{u}_k) + \omega_l(\mathbf{u}_k \times \mathbf{u}_j) + \omega_k(\mathbf{u}_j \times \mathbf{u}_l)) \cdot (\mathbf{u}_j \times \mathbf{u}_l) \geq 0 \quad (20c)$$

From inequality (15a), we get

$$\omega_i(\mathbf{u}_j \times \mathbf{u}_k)^2 \geq -\omega_j(\mathbf{u}_k \times \mathbf{u}_i) \cdot (\mathbf{u}_j \times \mathbf{u}_k) - \omega_k(\mathbf{u}_i \times \mathbf{u}_j) \cdot (\mathbf{u}_j \times \mathbf{u}_k)$$

and from inequality (20b), we get

$$\omega_l(\mathbf{u}_j \times \mathbf{u}_k)^2 \geq -\omega_j(\mathbf{u}_k \times \mathbf{u}_l) \cdot (\mathbf{u}_j \times \mathbf{u}_k) - \omega_k(\mathbf{u}_l \times \mathbf{u}_j) \cdot (\mathbf{u}_j \times \mathbf{u}_k)$$

From these, we get

$$\begin{aligned} & (\mathbf{u}_j \times \mathbf{u}_k)^2 (\omega_l[\mathbf{u}_i, \mathbf{u}_j, \mathbf{u}_k] - \omega_k[\mathbf{u}_i, \mathbf{u}_j, \mathbf{u}_l] + \omega_j[\mathbf{u}_i, \mathbf{u}_k, \mathbf{u}_l] + \omega_i[\mathbf{u}_j, \mathbf{u}_l, \mathbf{u}_k]) \\ & \geq \omega_j \left([\mathbf{u}_i, \mathbf{u}_k, \mathbf{u}_l] (\mathbf{u}_j \times \mathbf{u}_k)^2 - [\mathbf{u}_j, \mathbf{u}_l, \mathbf{u}_k] (\mathbf{u}_k \times \mathbf{u}_i) \cdot (\mathbf{u}_j \times \mathbf{u}_k) - [\mathbf{u}_i, \mathbf{u}_j, \mathbf{u}_k] (\mathbf{u}_k \times \mathbf{u}_l) \cdot (\mathbf{u}_j \times \mathbf{u}_k) \right) \\ & \quad - \omega_k \left([\mathbf{u}_i, \mathbf{u}_j, \mathbf{u}_l] (\mathbf{u}_j \times \mathbf{u}_k)^2 + [\mathbf{u}_j, \mathbf{u}_l, \mathbf{u}_k] (\mathbf{u}_i \times \mathbf{u}_j) \cdot (\mathbf{u}_j \times \mathbf{u}_k) + [\mathbf{u}_i, \mathbf{u}_j, \mathbf{u}_k] (\mathbf{u}_l \times \mathbf{u}_j) \cdot (\mathbf{u}_j \times \mathbf{u}_k) \right) \end{aligned}$$

This last term is equal to zero (see section B.4 for calculation details), which proves proposition 9.

6 Applications

6.1 Designing Chamfer masks

6.1.1 Building masks with Farey sets

Since the construction of Chamfer masks with Farey sets has been detailed in other publications (e.g. [35, 30]), we only recall here some necessary notions in 3-D (the restriction to the 2-D case is straightforward). A Farey set \mathcal{F}_n of order n correspond to the vectors of the Chamfer mask $n \times n \times n$ in the $1/48$ th of the space (the dark sector in figure 1).

The Farey set \mathcal{F}_1 of order 1, depicted in figure 1, is made of the 3 vectors $\left\{ \begin{pmatrix} 1 \\ 0 \\ 0 \end{pmatrix}, \begin{pmatrix} 1 \\ 1 \\ 0 \end{pmatrix}, \begin{pmatrix} 1 \\ 1 \\ 1 \end{pmatrix} \right\}$

and the corresponding triangulation, \mathcal{T}_1 consists in a single sector $\left\{ \left\langle \begin{pmatrix} 1 \\ 0 \\ 0 \end{pmatrix}, \begin{pmatrix} 1 \\ 1 \\ 0 \end{pmatrix}, \begin{pmatrix} 1 \\ 1 \\ 1 \end{pmatrix} \right\rangle \right\}$.

Large Chamfer masks, together with their triangulations, can be recursively build from a smaller one:

$$\mathcal{F}_{n+1} = \mathcal{F}_n \cup \left\{ \begin{pmatrix} x \\ y \\ z \end{pmatrix} + \begin{pmatrix} x' \\ y' \\ z' \end{pmatrix}, \text{ with } \max(x+x', y+y', z+z') \leq n+1, \text{ and } \begin{pmatrix} x \\ y \\ z \end{pmatrix}, \begin{pmatrix} x' \\ y' \\ z' \end{pmatrix} \in \mathcal{F}_n \right\} \quad (21)$$

More precisely, we sequentially consider the sectors $\langle \mathbf{n}_i, \mathbf{n}_j, \mathbf{n}_k \rangle$ of \mathcal{T}_n , and together with adding $\mathbf{n}_j + \mathbf{n}_k$ to \mathcal{F}_{n+1} , we replace the sector $\langle \mathbf{n}_i, \mathbf{n}_j, \mathbf{n}_k \rangle$ in \mathcal{T}_n with the two sectors $\langle \mathbf{n}_i, \mathbf{n}_j + \mathbf{n}_k, \mathbf{n}_k \rangle$ and $\langle \mathbf{n}_i, \mathbf{n}_j, \mathbf{n}_j + \mathbf{n}_k \rangle$, and, if there also exists a sector $\langle \mathbf{n}_j, \mathbf{n}_k, \mathbf{n}_l \rangle$ (as depicted in figure 4) in \mathcal{T}_n , it is splitted the same way. It can be proved that, if the sector $\langle \mathbf{n}_i, \mathbf{n}_j, \mathbf{n}_k \rangle$ is regular, then the newly built sectors are also regular [30].

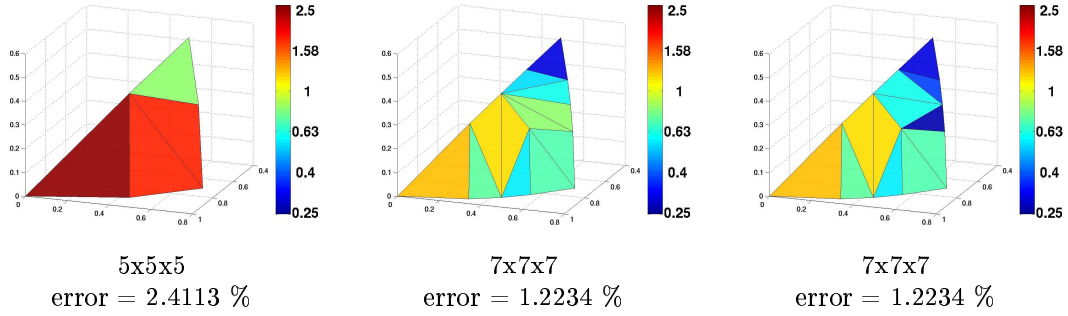


Figure 5: Errors (given in percentage) associated with the sectors of triangulated isotropic 3D chamfer masks (only 1/48th of the sphere built from the $\mathbf{n}/\|\mathbf{n}\|$ is depicted). From left to right, the triangulation of the 5x5x5 mask, the triangulation of the 7x7x7 mask as built in [30], and the triangulation of the 7x7x7 mask built by explicitly minimizing the error.

6.1.2 Optimal triangulations

When designing 3D Chamfer masks, it comes out that different triangulations can be built from the same set of vectors. Indeed, when a sector $\langle \mathbf{n}_i, \mathbf{n}_j, \mathbf{n}_k \rangle \in \mathcal{T}_n$ has to be splitted, we have to consider either the vector $\mathbf{n}_i + \mathbf{n}_j$, or $\mathbf{n}_j + \mathbf{n}_k$, or $\mathbf{n}_k + \mathbf{n}_i$, and more than one of them may belong to \mathcal{F}_{n+1} (see Eq. (21)), say for instance the first two.

If we consider $\mathbf{n}_i + \mathbf{n}_j$ as the vector to be added, then we create the two sectors $\langle \mathbf{n}_i + \mathbf{n}_j, \mathbf{n}_j, \mathbf{n}_k \rangle$ and $\langle \mathbf{n}_i, \mathbf{n}_i + \mathbf{n}_j, \mathbf{n}_k \rangle$. Conversely, if we consider $\mathbf{n}_j + \mathbf{n}_k$ as the vector to be added, then we create the two sectors $\langle \mathbf{n}_i, \mathbf{n}_j + \mathbf{n}_k, \mathbf{n}_k \rangle$ and $\langle \mathbf{n}_i, \mathbf{n}_j, \mathbf{n}_j + \mathbf{n}_k \rangle$. Thus, depending on the order we add the vectors to \mathcal{F}_{n+1} , we may end up with different triangulations.

To decide between different possible choices, a heuristic geometric rule was proposed in [30], and this yield the 7x7x7 triangulation depicted in the middle of figure 5 (or \mathcal{T}_3 in figure 13 in [30]).

We propose here a more rigorous rule to choose between different vectors. We compute the best possible errors of the two sectors $\langle \mathbf{n}_i + \mathbf{n}_j, \mathbf{n}_j, \mathbf{n}_k \rangle$ and $\langle \mathbf{n}_i, \mathbf{n}_i + \mathbf{n}_j, \mathbf{n}_k \rangle$, that are related to the creation of $\mathbf{n}_i + \mathbf{n}_j$, and associated the maximum of the two of them to $\mathbf{n}_i + \mathbf{n}_j$. We do the same with $\mathbf{n}_j + \mathbf{n}_k$.

After these computations have been conducted for the different possible choices, we can explicitly choose to add the vector that will minimize the maximum of the (best possible) errors of the two generated sectors. We observe that it yield a more homogeneous distributed error: compare the upper right part of the 7x7x7 triangulation at right of figure 5 with the one at the middle.

6.1.3 Optimal Chamfer masks

Classically, Chamfer masks are built with respect to a neighborhood size (*i.e.* $3 \times 3 \times 3$, $5 \times 5 \times 5$ or $7 \times 7 \times 7$). By increasing the number of vectors, one will decrease the error with respect to the Euclidean distance but increases the algorithmic complexity (hence the computational time of the Chamfer distance map).

It may be then interesting either to build mask with respect to a given error, or with respect to the algorithmic complexity (more precisely with respect to the number of vectors in the mask). In both cases, starting from the simplest mask (the $3 \times 3 \times 3$ one), one only have to iteratively split the sector of maximal error until the desired mask error or number of vectors is reached.

Figure 6 depicts the errors associated with anisotropic chamfer masks of different size, ranging from $3 \times 3 \times 3$ to $5 \times 5 \times 5$ (from [30]). A certain error discrepancy can be observed for each mask.

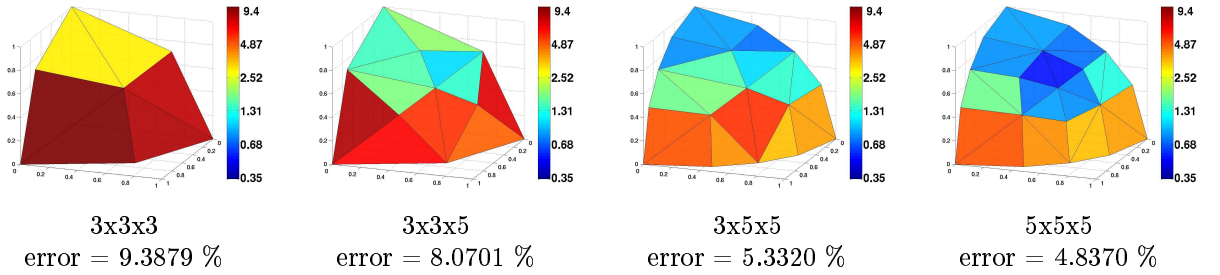


Figure 6: Errors (given in percentage) associated with the sectors of triangulated anisotropic 3D chamfer masks ($s_x = 1$, $s_y = 1.2$, $s_z = 2$). $1/8$ th of the sphere built from the $\mathbf{n}/\|\mathbf{n}\|$ is depicted.

The $3 \times 3 \times 5$ (left of figure 6) mask has 10 vectors in the $1/8$ th of the space. As proposed above, a 10 vectors mask can also be built by iteratively splitting the sector of maximal error (left of figure 7). It can be then observed that using vector $\begin{pmatrix} 2 \\ 0 \\ 1 \end{pmatrix}$ instead of $\begin{pmatrix} 1 \\ 1 \\ 2 \end{pmatrix}$ yields a better error for the same computational cost of the associated distance map.

The same still holds for mask of larger size. The $3 \times 5 \times 5$ mask has 16 vectors. A mask built with the same number of vectors within the $5 \times 5 \times 5$ neighborhood will have a smaller error if the vector $\begin{pmatrix} 2 \\ 2 \\ 1 \end{pmatrix}$ is preferred to vector $\begin{pmatrix} 1 \\ 0 \\ 2 \end{pmatrix}$. Moreover, this mask has the same maximal error than the $5 \times 5 \times 5$ mask, but with a smaller computational cost.

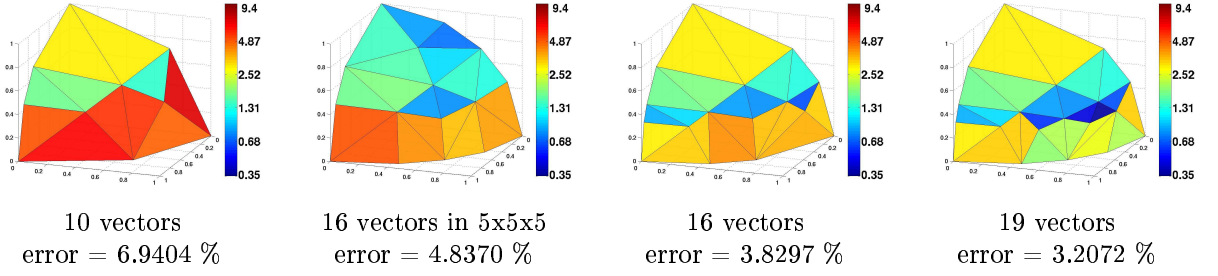


Figure 7: Errors (given in percentage) associated with the sectors of triangulated anisotropic 3D chamfer masks ($s_x = 1$, $s_y = 1.2$, $s_z = 2$). The mask vectors are chosen so that the mask error always decreases.

An even smaller error can be reached if the vectors are not constrained to belong to the 5x5x5 neighborhood. In this case, it can be observed that vectors $\left\{ \begin{pmatrix} 2 \\ 2 \\ 1 \end{pmatrix}, \begin{pmatrix} 3 \\ 1 \\ 1 \end{pmatrix}, \begin{pmatrix} 1 \\ 3 \\ 1 \end{pmatrix}, \begin{pmatrix} 3 \\ 0 \\ 1 \end{pmatrix} \right\}$

are preferred to vectors $\left\{ \begin{pmatrix} 1 \\ 0 \\ 2 \end{pmatrix}, \begin{pmatrix} 1 \\ 1 \\ 2 \end{pmatrix}, \begin{pmatrix} 1 \\ 2 \\ 0 \end{pmatrix}, \begin{pmatrix} 0 \\ 1 \\ 2 \end{pmatrix} \right\}$.

Finally, an optimal mask of 19 vectors (same complexity than the 5x5x5 mask) will use the vectors $\left\{ \begin{pmatrix} 3 \\ 1 \\ 1 \end{pmatrix}, \begin{pmatrix} 1 \\ 3 \\ 1 \end{pmatrix}, \begin{pmatrix} 3 \\ 0 \\ 1 \end{pmatrix}, \begin{pmatrix} 3 \\ 2 \\ 1 \end{pmatrix}, \begin{pmatrix} 2 \\ 3 \\ 1 \end{pmatrix} \right\}$ and will achieve the same maximal error than the 7x7x7 mask (49 vectors in the 1/8th of the space).

Moreover, it can be observed that the error range is less extended for the masks of figure 7 than of figure 6.

6.2 Computing optimal integer weights

In previous section, we discussed the design of Chamfer masks. As already mentioned, we are able to exhibit a set of real-valued weights that realizes the best possible error for a given mask.

However, we may be interested not in real-valued weights, but in integer-valued ones that we denote by \bar{w}_i . For a given set of integer weights, one compute both the minimum and the maximum values, \bar{D}_{min} and \bar{D}_{max} (see sections 3.1 and 4.1), of the Chamfer map, and we retrieve a set of real-valued weights by $w_i = \bar{w}_i / \varepsilon$ with $\varepsilon = (\bar{D}_{min} + \bar{D}_{max}) / 2$.

The point is now to calculate sets of optimal integer weights. We will consider a sorted list of couple $(\bar{w}_i, \mathbf{n}_i)$. The first (2 or 3, depending on the space dimension) couples are the ones that define the sector of maximal error. The rest of the list is built by adding the vector that allow to build a sector adjacent to the ones already defined by the vectors in the list

$\begin{smallmatrix} 1 \\ 0 \\ 0 \end{smallmatrix}$	$\begin{smallmatrix} 1 \\ 1 \\ 0 \end{smallmatrix}$	$\begin{smallmatrix} 1 \\ 1 \\ 1 \end{smallmatrix}$	$\begin{smallmatrix} 2 \\ 1 \\ 0 \end{smallmatrix}$	$\begin{smallmatrix} 2 \\ 1 \\ 1 \end{smallmatrix}$	$\begin{smallmatrix} 2 \\ 2 \\ 1 \end{smallmatrix}$	error	% / opt	ε	time
1	1	1	2	2	2	26.79	1111.2	0.789	0 ms
1	2	2	3	3	4	17.16	711.5	1.207	10 ms
2	3	3	5	5	6	12.70	526.8	1.984	10 ms
2	3	4	5	6	7	10.10	418.9	2.225	10 ms
3	4	5	7	7	9	5.57	231.1	2.995	10 ms
4	6	7	9	10	13	4.29	178.1	4.179	10 ms
5	7	9	11	12	15	2.94	122.1	5.048	20 ms
9	13	16	20	22	28	2.66	110.5	9.189	30 ms
11	16	20	25	27	34	2.55	105.8	11.288	30 ms
20	29	35	45	49	62	2.44	101.2	20.500	50 ms

Table 1: 5x5x5 Chamfer mask coefficients (isotropic case). The best possible error is 2.4113 %. The four last columns indicates the actual error, the percentage w.r.t. the best possible error, the multiplicative constant, and the computational time.

(so that additional convexity constraints can be test as soon as a weight is defined for this vector).

Assume that we are looking for the weight sets that verify $\bar{w}_{\mathbf{x}} \in [\bar{w}_{min}, \bar{w}_{max}]$. The weights \bar{w}_i of the 2 or 3 first vectors of the list are allowed to vary in $[\lfloor \bar{w}_{min} \|\mathbf{v}_i\|_{\infty} \rfloor, \lceil \bar{w}_{max} \|\mathbf{v}_i\|_1 \rceil]$.

For any doublet (or triplet) of weights, the minimum and maximum values, \hat{D}_{min} and \hat{D}_{max} , as well as $\hat{\varepsilon}$ are calculated. This allows to compute the error $\hat{E} = \hat{D}_{max} / \hat{\varepsilon} - 1$ of this sector. If this error is better than a previously computed error \hat{E}_p , the other vectors are considered.

The range of variation of the weights \bar{w}_k of these vectors could be constrained by the estimated error \hat{E} . It appears that it is too strict, since the minimum and maximum values of the distance map may not occur in the first cone, and we prefer to constrain it by previously computed error \hat{E}_p , yielding the range a variation $[\lfloor \hat{\varepsilon}(1 - \hat{E}_p) \|\mathbf{v}_k\| \rfloor, \lceil \hat{\varepsilon}(1 + \hat{E}_p) \|\mathbf{v}_k\| \rceil]$. This drastically reduces the depth-first search in the sets of possible integer weights. As in [30], alpha pruning is performed that consists in checking convexity criteria for each newly tested weight.

Once a complete set of integer weights have been identified, its error as well as its multiplicative constant ε are re-estimated. In addition, the percentage of error with respect to the best possible error (*i.e.* the error limit) can also computed: this may offer a mean to control and stop the coefficient computation.

Tables 1 and 2 give the optimal Chamfer coefficients for respectively the 5x5x5 and the 7x7x7 Chamfer masks (isotropic case). The estimated errors can not be directly compared to [30], since the error definition is different, but it can be noticed that they are comparable. A drastic reduction of the computational time can be observed.

Tables 3, 4, and 5, as well as tables 6, 7, and 8 give the optimal integer coefficients for the three first masks depicted in respectively figures 6 and 7.

1 0 0	1 1 0	1 1 1	2 1 0	2 1 1	2 2 1	3 1 0	3 2 0	3 1 1	3 2 1	3 3 1	3 2 2	3 3 2	error	% / opt	ϵ	time
1	1	1	2	2	2	3	3	3	3	3	3	3	26.79	2190.1	0.789	0 ms
1	2	2	3	3	4	4	5	4	5	6	5	6	17.16	1402.4	1.207	0 ms
2	3	3	5	5	6	7	8	7	8	9	8	9	12.70	1038.2	1.984	0 ms
2	3	4	5	6	7	7	8	8	9	10	10	11	10.10	825.7	2.225	0 ms
3	4	5	6	7	9	9	10	9	11	13	12	14	5.57	455.5	2.842	10 ms
4	6	7	9	10	13	13	15	13	16	19	17	20	5.31	433.7	4.139	10 ms
4	6	7	9	10	12	13	15	14	15	18	17	19	2.94	240.6	4.121	20 ms
7	10	12	16	17	21	22	26	23	27	31	29	33	2.48	202.4	7.104	30 ms
8	11	14	18	19	24	25	29	26	30	35	33	38	2.31	189.1	7.940	40 ms
9	13	16	20	22	27	29	33	30	34	40	38	43	1.81	147.8	9.109	50 ms
14	20	24	31	34	42	44	51	46	53	62	58	66	1.76	143.8	14.105	90 ms
17	24	30	38	42	52	54	61	57	65	76	71	81	1.75	143.1	17.220	150 ms
17	24	30	38	42	51	54	62	57	65	75	70	80	1.60	130.5	17.246	150 ms

Table 2: 7x7x7 Chamfer mask coefficients (isotropic case). The best possible error is 1.2234 %. The four last columns indicates the actual error, the percentage w.r.t. the best possible error, the multiplicative constant, and the computational time.

7 Conclusion

We have described and calculated the error between the Chamfer distance and the Euclidean one within a sector (defined respectively by two and three vectors in 2-D and in 3-D), estimated on a circle (or on a sphere). We have also provided closed forms for this error (sections 3.1 and 4.1).

This allowed us to compute the best possible error for each sector, and hence for the Chamfer mask, and to exhibit a set of optimal real-valued weights. These calculations are valid for any 2-D or 3-D lattice. This best possible error is then the lower limit of the errors induced by integer valued weights.

Having an error estimation defined locally allowed us to study the usual Chamfer masks (in \mathbb{Z}^3) that are built symmetrically with geometric considerations. It appeared that the error is inhomogeneously distributed on these masks.

We then proposed a new Chamfer mask construction method that iteratively add vectors to subdivide the sector of highest error. It allowed to build mask of given complexity (*i.e.* number of vectors) or given error (with the lowest complexity), with a more homogeneously distributed error.

Finally, by assuming that the error computed in the sector of highest error in a mask is a good estimate of the mask error itself, we proposed a new method to compute sets of optimal integer weights¹, that clearly outperform a previously proposed method [30].

¹The code used to build masks and to compute integer weights is available at <http://www-sop.inria.fr/epidaure/personnel/Gregoire.Malandain/codes/chamfer-coefficients.html>

1 0 0	0 1 0	0 1 1	1 1 0	1 0 1	0 1 1	1 1 1	error	% / opt	ε	time
1	1	1	1	2	2	2	38.20	406.9	0.809	0 ms
1	1	2	1	2	2	2	27.18	289.5	0.879	0 ms
1	1	2	2	2	2	2	24.58	261.8	1.045	0 ms
2	2	3	3	4	4	4	19.70	209.9	1.868	10 ms
2	2	4	3	4	4	4	17.31	184.4	1.906	10 ms
2	3	4	3	5	5	5	16.74	178.3	2.307	10 ms
2	3	4	4	5	5	5	16.32	173.8	2.354	10 ms
3	3	5	4	6	6	7	16.05	171.0	2.978	10 ms
3	4	6	5	6	7	7	15.33	163.3	3.169	10 ms
3	4	6	5	7	7	7	13.98	149.0	3.207	10 ms
3	4	6	5	7	7	8	11.63	123.9	3.395	10 ms
4	5	8	6	9	9	10	10.99	117.1	4.316	20 ms
5	6	10	8	11	12	13	10.91	116.2	5.522	20 ms
5	6	10	8	12	12	13	10.39	110.7	5.580	20 ms
7	9	14	11	16	17	18	10.02	106.7	7.779	30 ms
9	11	18	14	20	21	23	9.81	104.5	9.918	30 ms
13	16	26	21	30	31	33	9.70	103.4	14.397	50 ms
15	18	30	24	34	35	38	9.65	102.8	16.573	60 ms
16	20	32	25	36	38	41	9.60	102.2	17.699	70 ms

Table 3: 3x3x3 Chamfer mask coefficients (anisotropic case, $s_x = 1$, $s_y = 1.2$, $s_z = 2$) that correspond to the first mask of figure 6. The best possible error is 9.3879 %. The four last columns indicates the actual error, the percentage w.r.t. the best possible error, the multiplicative constant, and the computational time.

1 0 0	0 1 0	0 0 1	1 1 0	1 0 1	0 1 1	1 1 1	2 1 1	1 2 1	1 1 2	error	% / opt	ϵ	time
1	1	1	1	2	1	2	3	2	3	44.56	552.2	0.773	0 ms
1	1	1	1	2	2	2	3	3	3	38.20	473.3	0.809	0 ms
1	1	2	1	2	2	2	3	3	4	27.18	336.8	0.879	0 ms
1	1	2	2	2	2	2	3	3	4	24.58	304.5	1.045	0 ms
2	2	3	2	3	3	4	5	5	6	23.38	289.7	1.671	10 ms
2	2	3	3	4	4	4	6	6	7	19.70	244.1	1.868	10 ms
2	2	4	3	4	4	4	6	6	8	17.31	214.5	1.906	10 ms
2	2	4	3	4	4	5	6	7	8	14.59	180.8	1.951	10 ms
3	4	6	5	7	7	7	10	11	13	13.98	173.3	3.207	20 ms
3	4	6	5	7	7	8	10	11	13	9.85	122.0	3.328	20 ms
5	6	10	8	11	12	13	16	18	22	8.48	105.1	5.375	40 ms
8	10	16	13	18	19	21	26	29	35	8.42	104.3	8.735	70 ms
9	11	18	14	20	21	23	29	32	39	8.23	101.9	9.746	100 ms
17	21	34	27	38	40	43	55	61	74	8.22	101.9	18.463	390 ms
17	21	34	27	38	40	44	55	61	74	8.08	100.1	18.488	440 ms

Table 4: 3x3x5 Chamfer mask coefficients (anisotropic case, $s_x = 1$, $s_y = 1.2$, $s_z = 2$) that correspond to the second mask of figure 6. The best possible error is 8.0701 %. The four last columns indicates the actual error, the percentage w.r.t. the best possible error, the multiplicative constant, and the computational time.

1	0	0	1	1	0	1	2	2	1	0	0	2	1	1	error	% / opt	ϵ	time		
0	1	0	1	0	1	1	1	0	2	0	2	1	2	1						
0	0	1	0	1	1	1	0	1	0	2	1	2	1	1						
1	1	1	1	1	2	2	2	2	2	3	3	2	3	3	38.20	716.4	0.724	0 ms		
1	1	2	1	2	2	2	2	2	2	4	3	4	2	3	4	21.94	411.4	0.820	0 ms	
2	2	3	3	3	4	4	4	4	5	5	6	6	5	6	6	21.15	396.7	1.702	20 ms	
2	2	3	3	4	4	4	4	4	5	5	7	6	7	5	6	7	15.77	295.7	1.781	20 ms
2	2	4	3	4	4	4	4	4	5	5	8	6	8	5	6	8	13.34	250.2	1.819	20 ms
3	3	5	4	6	6	7	7	7	7	11	9	11	8	10	12	12.06	226.1	2.814	40 ms	
3	3	5	4	6	6	7	6	8	7	11	9	11	8	10	12	11.70	219.4	2.831	40 ms	
3	4	6	5	7	7	7	7	9	8	12	10	12	9	10	12	11.57	217.0	3.119	60 ms	
3	4	6	5	7	7	8	7	9	9	12	10	13	10	11	13	10.88	204.0	3.266	70 ms	
3	4	6	5	7	7	8	7	9	9	13	10	13	10	11	13	9.38	175.9	3.310	70 ms	
4	5	8	6	9	9	10	9	11	11	16	13	17	12	14	17	8.34	156.4	4.191	130 ms	
5	6	10	8	11	11	12	11	14	13	20	16	21	15	17	21	7.76	145.6	5.113	450 ms	
5	6	10	8	11	12	13	12	14	13	21	17	21	16	18	21	7.74	145.1	5.300	500 ms	
5	6	10	8	11	12	13	12	14	13	21	17	21	16	18	22	7.44	139.6	5.315	520 ms	
5	6	10	8	12	12	13	12	15	13	21	17	21	16	18	22	6.63	124.4	5.355	540 ms	
9	11	18	14	20	21	23	21	26	24	37	30	38	28	32	39	6.56	123.0	9.572	23.43 s	
9	11	18	14	21	21	23	21	26	24	37	30	38	28	32	39	6.45	121.1	9.581	24.10 s	
9	11	18	14	20	21	23	21	26	24	37	29	38	29	31	39	6.37	119.5	9.553	27.24 s	
12	15	24	19	27	28	31	28	35	33	50	39	51	39	42	52	6.32	118.6	12.810	7 min 40 s	
12	15	24	19	27	28	31	28	35	32	50	40	51	39	42	52	6.30	118.2	12.807	7 min 40 s	
13	16	26	21	30	31	33	31	39	34	54	43	55	42	45	56	6.30	118.1	13.874	17 min	
14	17	28	22	31	33	35	33	40	36	57	46	59	44	48	60	6.18	115.9	14.700	31 min	
14	17	28	22	32	33	36	33	41	37	58	46	59	45	49	60	6.11	114.6	14.882	37 min	
14	17	28	22	32	33	36	33	41	37	58	46	59	45	49	61	6.01	112.8	14.896	37 min	
15	18	30	24	34	35	38	35	44	39	62	49	63	48	52	65	6.00	112.5	15.930	1 h 2 min	
17	21	34	27	38	40	43	40	49	45	70	56	71	54	59	73	5.94	111.4	18.015	3 h 17 min	
19	23	38	30	43	44	48	44	55	50	78	62	79	60	66	81	5.90	110.6	20.045	6 h 46 min	
19	23	38	30	43	44	48	44	55	50	78	62	80	60	66	82	5.89	110.5	20.046	6 h 46 min	
19	23	38	30	43	45	48	45	55	50	78	63	80	60	66	82	5.80	108.8	20.079	6 h 46 min	

Table 5: 3x5x5 Chamfer mask coefficients (anisotropic case, $s_x = 1$, $s_y = 1.2$, $s_z = 2$) that correspond to the third mask of figure 6. The best possible error is 5.3320 %. The four last columns indicates the actual error, the percentage w.r.t. the best possible error, the multiplicative constant, and the computational time.

1 0 0	0 1 0	0 0 1	1 1 0	1 0 1	0 1 1	1 1 1	2 0 1	2 1 1	1 2 1	error	% / opt	ϵ	time
1	1	1	1	1	2	2	2	2	3	38.20	550.3	0.724	0 ms
1	1	2	1	2	2	2	2	2	3	21.94	316.1	0.820	0 ms
2	2	3	3	4	4	4	5	5	6	18.18	262.0	1.833	10 ms
2	2	4	3	4	4	4	5	5	6	15.78	227.3	1.871	10 ms
2	2	4	3	5	4	5	6	6	7	14.59	210.2	1.951	10 ms
3	3	5	4	6	6	6	8	8	9	14.44	208.0	2.763	10 ms
3	3	5	4	6	6	7	8	9	9	13.35	192.3	2.885	10 ms
3	3	5	4	6	6	7	7	8	10	12.06	173.7	2.814	20 ms
3	3	5	4	6	6	7	8	8	10	11.70	168.5	2.831	20 ms
3	4	6	5	7	7	8	9	10	11	9.85	141.9	3.328	20 ms
4	5	8	6	9	9	10	11	12	14	9.22	132.9	4.231	30 ms
5	6	10	8	11	12	13	14	16	18	8.48	122.2	5.375	50 ms
5	6	10	8	12	12	13	15	16	18	7.67	110.5	5.415	50 ms
9	11	18	14	21	21	23	26	28	32	7.62	109.8	9.702	130 ms
10	12	20	16	22	23	25	28	31	35	7.60	109.5	10.648	170 ms
10	12	20	16	23	23	25	29	31	35	7.53	108.5	10.654	170 ms
11	13	22	17	25	25	28	31	34	39	7.47	107.7	11.584	270 ms
15	18	30	24	34	35	38	43	47	53	7.04	101.4	16.108	1.11 s

Table 6: 10 vectors Chamfer mask coefficients (anisotropic case, $s_x = 1$, $s_y = 1.2$, $s_z = 2$) that correspond to the first mask of figure 7. The best possible error is 6.9404 %. The four last columns indicates the actual error, the percentage w.r.t. the best possible error, the multiplicative constant, and the computational time.

	1	0	0	1	1	0	1	2	2	1	0	0	2	1	1	2	error	% / opt	ϵ	time
1	0	0	1	1	0	1	1	1	0	2	2	1	1	2	1	2	43.47	898.6	0.697	0 ms
1	1	0	1	0	1	1	1	0	1	0	2	2	1	2	1	2	29.94	619.0	0.770	0 ms
1	1	1	1	1	1	1	1	2	2	2	2	2	2	2	2	2	21.94	453.5	0.820	0 ms
2	2	3	3	3	4	4	4	5	5	6	6	5	6	6	7	7	21.15	437.3	1.702	20 ms
2	2	3	3	4	4	4	4	5	5	6	7	5	6	7	7	7	15.77	326.0	1.781	20 ms
2	2	4	3	4	4	4	4	5	5	6	8	5	6	8	7	7	13.34	275.8	1.819	20 ms
3	3	5	4	6	6	7	6	8	7	8	11	8	9	12	10	11	11.70	241.8	2.831	30 ms
3	4	6	5	7	7	7	7	9	8	10	13	9	10	13	12	11	11.57	239.2	3.119	60 ms
3	4	6	5	7	7	8	7	9	9	10	13	9	11	14	12	10	10.56	218.3	3.275	60 ms
3	4	6	5	7	7	8	7	9	9	10	13	10	11	13	13	9	9.38	193.9	3.310	70 ms
3	4	6	5	7	7	8	8	9	9	10	13	9	10	14	11	9	9.10	188.2	3.223	70 ms
3	4	6	5	7	7	8	8	9	8	10	13	10	10	13	12	8	8.74	180.7	3.287	80 ms
4	5	8	6	9	9	10	9	11	11	12	16	12	13	17	15	6	6.91	142.9	4.116	140 ms
4	5	8	6	9	9	10	9	11	11	12	17	12	13	17	15	6	6.78	140.2	4.121	140 ms
5	6	10	8	11	12	13	12	14	14	16	21	15	17	22	19	6	6.76	139.8	5.236	240 ms
5	6	10	8	12	12	13	12	15	13	16	21	16	17	22	20	6	6.12	126.5	5.326	360 ms
7	9	14	11	16	17	18	17	20	19	22	29	22	23	30	27	6	6.07	125.5	7.393	2.01 s
7	9	14	11	16	17	18	17	20	19	22	30	22	23	30	27	5	5.77	119.3	7.414	2.01 s
7	9	14	11	16	17	18	17	20	19	22	30	22	23	31	27	5	5.67	117.3	7.421	2.01 s
9	11	18	14	20	21	23	21	26	24	28	38	28	30	39	35	5	5.52	114.1	9.467	7.91 s
9	11	18	14	21	21	23	21	26	24	28	38	28	30	39	35	5	5.42	112.0	9.476	7.91 s
10	12	20	16	23	24	26	24	29	27	32	42	31	34	44	39	5	5.24	108.4	10.553	12.48 s
12	15	24	19	27	28	31	29	34	32	38	51	37	40	52	46	5	5.20	107.6	12.659	46.69 s
13	16	26	21	29	31	33	31	37	35	42	55	40	44	56	51	5	5.19	107.3	13.679	1 min 7 s
13	16	26	21	30	31	33	31	37	35	42	55	40	44	56	51	5	5.07	104.8	13.694	1 min 7 s
14	17	28	22	32	33	36	33	40	37	44	59	43	47	61	54	4	4.90	101.4	14.717	1 min 41 s

Table 7: 16 vectors (constrained in the 5x5x5 neighborhood) Chamfer mask coefficients (anisotropic case, $s_x = 1$, $s_y = 1.2$, $s_z = 2$) that correspond to the second mask of figure 7. The best possible error is 4.8370 %. The four last columns indicates the actual error, the percentage w.r.t. the best possible error, the multiplicative constant, and the computational time.

	1	0	0	1	1	0	1	2	2	0	2	1	2	3	3	1	error	% / opt	ϵ	time
1	0	0	1	1	0	1	1	1	0	2	2	1	2	2	3	3	43.47	1135.0	0.697	0 ms
1	1	1	1	1	1	2	2	2	2	3	2	3	3	3	3	4	38.20	997.4	0.724	0 ms
1	1	2	1	2	2	2	2	2	2	2	2	2	2	3	3	3	29.94	781.8	0.770	0 ms
1	1	2	1	2	2	2	2	2	2	3	2	3	3	3	3	4	21.94	572.8	0.820	0 ms
2	2	3	3	3	4	4	4	4	6	5	6	7	6	6	8	8	19.87	518.8	1.674	20 ms
2	2	3	3	4	4	4	4	5	6	5	6	7	6	6	8	8	14.46	377.5	1.753	20 ms
2	2	4	3	4	4	4	4	5	6	5	6	7	6	6	8	8	12.02	313.9	1.792	20 ms
3	3	5	4	6	6	7	6	7	8	8	9	10	10	10	12	10	10.27	268.2	2.758	40 ms
3	3	5	4	6	6	7	6	8	8	8	9	10	10	10	12	9	9.77	255.1	2.771	40 ms
3	4	6	5	7	7	8	7	9	10	10	11	13	11	12	14	8	8.19	214.0	3.268	70 ms
4	5	8	6	9	9	10	9	11	12	12	13	15	14	15	17	5	5.80	151.4	4.078	120 ms
5	6	10	8	12	12	13	12	15	16	16	17	20	19	20	22	5	5.46	142.6	5.289	250 ms
6	7	12	9	13	14	15	14	17	18	18	19	22	22	23	25	5	5.29	138.1	6.083	370 ms
8	9	15	12	17	18	19	18	22	24	23	25	29	28	29	33	5	5.21	136.0	7.897	1.46 s
9	11	18	14	20	21	23	21	25	28	28	30	35	32	35	39	4	4.96	129.5	9.300	4.73 s
9	11	18	14	20	21	23	21	26	28	28	30	35	33	35	39	4	4.37	114.0	9.353	4.83 s
9	11	18	14	21	21	23	21	26	28	28	30	35	33	35	39	4	4.26	111.4	9.362	4.84 s
17	20	33	26	37	39	42	39	47	52	51	55	64	60	64	72	4	4.25	111.1	17.233	2 min 27 s
17	20	34	26	37	39	42	39	47	52	51	55	64	60	64	72	4	4.11	107.4	17.256	2 min 27 s
17	20	34	26	38	39	42	39	47	52	51	55	64	60	64	72	4	4.10	107.1	17.258	2 min 27 s

Table 8: 16 vectors Chamfer mask coefficients (anisotropic case, $s_x = 1$, $s_y = 1.2$, $s_z = 2$) that correspond to the third mask of figure 7. The best possible error is 3.8297 %. The four last columns indicates the actual error, the percentage w.r.t. the best possible error, the multiplicative constant, and the computational time.

References

- [1] J. Serra. *Image Analysis and Mathematical Morphology*. Academic Press, 1982.
- [2] Pierre Soille. *Morphological image analysis: principles and applications*. Springer, 1999.
- [3] B. Kruse. An exact sequential euclidean distance algorithm with application to skeletonizing. In *7th Scandinavian Conference on Image Analysis (SCIA '91)*, pages 982–992, 1991.
- [4] Chris J. Pudney. Distance-ordered homotopic thinning: A skeletonization algorithm for 3D digital images. *Computer Vision and Image Understanding*, 72(3):404–413, December 1998.
- [5] Gabor T. Herman, Jingsheng Zheng, and Carolyn A. Bucholtz. Shape-based interpolation. *IEEE Computer Graphics & Applications*, 12(3):69–79, May 1992.
- [6] George J. Grevera and Jayaram K. Udupa. Shape-based interpolation of multidimensional grey-level images. *IEEE Transactions on Medical Imaging*, 15(6):881–892, December 1996.
- [7] D. Cohen-Or, D. Levin, and A. Solomovici. Three dimensional distance field metamorphosis. *ACM Transactions of Graphics*, 17(2):116–141, 1998.
- [8] G. Borgefors. Hierarchical chamfer matching: A parametric edge matching algorithm. *IEEE Transactions on Pattern Analysis and Machine Intelligence*, 10(6):849–865, november 1988.
- [9] M van Herk and H M Kooy. Automatic three-dimensional correlation of CT-CT, CT-MRI, and CT-SPECT using chamfer matching. *Med Phys*, 21(7):1163–78, July 1994.
- [10] Stina Svensson and G. Sanniti di Baja. Using distance transforms to decompose 3d discrete objects. *Image and Vision Computing*, 20:529–540, 2002.
- [11] P.E. Danielsson. Euclidean distance mapping. *Computer Graphics and Image Processing*, 14(3):227–248, 1980.
- [12] Q.Z. Ye. The signed euclidean distance transform and its applications. In *International Conference on Pattern Recognition*, pages 495–499, 1988.
- [13] Ingemar Ragnemalm. The euclidean distance transform in arbitrary dimensions. *Pattern Recognition Letters*, 14(11):883–888, November 1993.
- [14] T. Saito and J.i. Toriwaki. New algorithms for euclidean distance transformation of an n-dimensional digitized picture with applications. *Pattern Recognition*, 27(11):1551–1565, 1994.

- [15] C.T. Huang and O.R. Mitchell. A euclidean distance transform using grayscale morphology decomposition. *IEEE transactions on Pattern Analysis and Machine Intelligence*, 16(4):443–448, April 1994.
- [16] Tomio Hirata. A unified linear-time algorithm for computing distance maps. *Information Processing Letters*, 58(3):129–133, 1996.
- [17] A. Meijster, J.B.T.M. Roerdink, and W.H. Hesselink. A general algorithm for computing distance transforms in linear time. In J. Goutsias, L. Vincent, and D.S. Bloomberg, editors, *Mathematical Morphology and its Applications to Image and Signal Processing*, pages 331–340. Kluwer, 2000.
- [18] Calvin R. Maurer, Rensheng Qi, and Vijay Raghavan. A linear time algorithm for computing exact euclidean distance transforms of binary images in arbitrary dimensions. *IEEE Transactions on Pattern Analysis and Machine Intelligence*, 25(2):265–270, 2003.
- [19] George J. Grevera. The "dead reckoning" signed distance transform. *Computer Vision and Image Understanding*, 95(3):317–333, 2004.
- [20] Céline Fouard, Grégoire Malandain, Stefen Prohaska, Malte Westerhoff, Francis Casot, Christophe Mazel, Didier Asselot, and Jean-Pierre Marc-Vergnes. Skeletonization by blocks for large datasets: application to brain microcirculation. In *International Symposium on Biomedical Imaging: From Nano to Macro (ISBI'04)*, Arlington, VA, USA, April 2004. IEEE.
- [21] A. Rosenfeld and J.L. Pfaltz. Sequential operations in digital picture processing. *Journal of the Association for Computing Machinery*, 13(4):471–494, October 1966.
- [22] U. Montanari. A method for obtaining skeletons using a quasi-euclidean distance. *Journal of the Association for Computing Machinery*, 15:600–624, 1968.
- [23] G. Borgefors. Distance transformations in arbitrary dimensions. *Computer Vision, Graphics, and Image Processing*, 27:321–345, February 1984.
- [24] G. Borgefors. Distance transformations in digital images. *Computer Vision, Graphics, and Image Processing*, 34(3):344–371, February 1986.
- [25] G. Borgefors. On digital distance transforms in three dimensions. *Computer Vision and Image Understanding*, 64(3):368–376, November 1996.
- [26] J.F. Mangin, I. Bloch, J. López-Krahe, and V. Frouin. Chamfer distances in anisotropic 3D images. In *VII European Signal Processing Conference*, Edimburgh, UK, september 1994.
- [27] D. Coquin, Y. Chehadeh, and P. Bolon. 3d local distance operator on parallelepipedic grids. In *Proc. 4th Discrete Geometry for Computer Imagery*, pages 147–156, Grenoble, France, 1994.

- [28] Ida-Maria Sintorn and Gunilla Borgefors. Weighted distance transforms for volume images digitized in elongated voxel grids. *Pattern Recognition Letters*, 25(5):571–580, 2004.
- [29] J F Mangin, V Frouin, I Bloch, B Bendriem, and J Lopez-Krahe. Fast nonsupervised 3D registration of PET and MR images of the brain. *J Cereb Blood Flow Metab*, 14(5):749–62, September 1994.
- [30] Céline Fouard and Grégoire Malandain. 3-d chamfer distances and norms in anisotropic grids. *Image and Vision Computing*, 23(2):143–158, February 2005.
- [31] Christer O. Kiselman. Regularity properties of distance transformations in image analysis. *Computer Vision and Image Understanding*, 64(3):390–398, 1996.
- [32] B.J.H Verwer. Local distances for distance transformations in two and three dimensions. *Pattern Recognition Letters*, 12:671–682, November 1991.
- [33] E. Remy and E. Thiel. Optimizing 3d chamfer masks with norm constraints. In *International Workshop on Combinatorial Image Analysis*, pages 39–56, July 2000.
- [34] E. Remy. *Normes de chanfrein et axe médian dans le volume discret*. PhD thesis, Université de la Méditerranée, Marseille, France, December 2001.
- [35] E. Thiel. *Géométrie des distances de chanfrein*. Habilitation à diriger des recherches, Université de la Méditerranée (Aix-Marseille II), 2001.

A The 2-D case

A.1 Error extrema

The coordinates of the points M_a and M_b are respectively $M_a = (x_a, y_a) = (x_i R / \|\mathbf{v}_i\|, y_i R / \|\mathbf{v}_i\|)$ and $M_b = (x_b, y_b) = (x_j R / \|\mathbf{v}_j\|, y_j R / \|\mathbf{v}_j\|)$. We obtain for the error values at these points

$$\begin{aligned} E(M_a) &= \alpha x_a + \beta y_a - R \\ &= \frac{x_i(y_j w_i - y_i w_j) + y_i(-x_j w_i + x_i w_j)}{(\mathbf{n}_i \times \mathbf{n}_j) \|\mathbf{v}_i\|} R - R \\ &= \frac{x_i y_j - x_j y_i}{(\mathbf{n}_i \times \mathbf{n}_j)} \frac{w_i}{\|\mathbf{v}_i\|} R - R = \omega_i R - R \end{aligned}$$

and

$$\begin{aligned} E(M_b) &= \alpha x_b + \beta y_b - R \\ &= \frac{x_j(y_j w_i - y_i w_j) + y_j(-x_j w_i + x_i w_j)}{(\mathbf{n}_i \times \mathbf{n}_j) \|\mathbf{v}_j\|} R - R \\ &= \frac{x_i y_j - x_j y_i}{(\mathbf{n}_i \times \mathbf{n}_j)} \frac{w_j}{\|\mathbf{v}_j\|} R - R = \omega_j R - R \end{aligned}$$

$$\begin{aligned} E(M_{ext}) &= \alpha x_{ext} + \beta y_{ext} - R \\ &= \frac{s_y^2}{s_x s_y} \frac{\alpha^2}{\sqrt{\beta^2 s_x^2 + \alpha^2 s_y^2}} R + \frac{s_x^2}{s_x s_y} \frac{\beta^2}{\sqrt{\beta^2 s_x^2 + \alpha^2 s_y^2}} R - R \\ &= \frac{1}{s_x s_y} \sqrt{\beta^2 s_x^2 + \alpha^2 s_y^2} R - R \end{aligned}$$

It can be noticed that $\beta^2 s_x^2 + \alpha^2 s_y^2 = \frac{\|w_i \mathbf{v}_j - w_j \mathbf{v}_i\|^2}{(\mathbf{n}_i \times \mathbf{n}_j)^2}$. Since $s_x s_y (\mathbf{n}_i \times \mathbf{n}_j) = \mathbf{v}_i \times \mathbf{v}_j$, we obtain

$$E(M_{ext}) = \frac{\|w_i \mathbf{v}_j - w_j \mathbf{v}_i\|}{\mathbf{v}_i \times \mathbf{v}_j} R - R$$

and after dividing both the numerator and the denominator of the fraction by $\|\mathbf{v}_i\| \|\mathbf{v}_j\|$, we finally obtain

$$E(M_{ext}) = \frac{\|\omega_i \mathbf{u}_j - \omega_j \mathbf{u}_i\|}{\mathbf{u}_i \times \mathbf{u}_j} R - R$$

A.2 Proof of proposition 1

M_{ext} lies within the sector $(O, \mathbf{u}_i, \mathbf{u}_j)$ iff we have $a_{ext} \geq 0$ and $b_{ext} \geq 0$, with a_{ext} and b_{ext} defined by replacing x and y in the expressions of both a and b (Eq. (1)) by x_{ext} and y_{ext} .

It comes

$$\begin{aligned}
a_{ext} \geq 0 &\iff x_{ext}y_j - x_jy_{ext} \geq 0 \iff s_y^2\alpha y_j - s_x^2\beta x_j \geq 0 \\
&\iff s_y^2y_j^2w_i - s_y^2y_iy_jw_j + s_x^2x_j^2w_i - s_x^2x_ix_jw_j \geq 0 \quad \text{recall that } \mathbf{n}_i \times \mathbf{n}_j \geq 0 \\
&\iff \frac{s_x^2x_j^2 + s_y^2y_j^2}{s_x^2x_ix_j + s_y^2y_iy_j} = \frac{\|\mathbf{v}_j\|^2}{\mathbf{v}_i \cdot \mathbf{v}_j} = \frac{1}{\mathbf{u}_i \cdot \mathbf{u}_j} \frac{\|\mathbf{v}_j\|}{\|\mathbf{v}_i\|} \geq \frac{w_j}{w_i} \\
&\iff \frac{1}{\mathbf{u}_i \cdot \mathbf{u}_j} \geq \frac{\omega_j}{\omega_i}
\end{aligned}$$

and

$$\begin{aligned}
b_{ext} \geq 0 &\iff x_iy_{ext} - y_ix_{ext} \geq 0 \iff s_x^2\beta x_i - s_y^2\alpha y_i \geq 0 \\
&\iff -s_x^2x_ix_jw_i + s_x^2x_i^2w_j - s_y^2y_iy_jw_i + s_y^2y_i^2w_j \geq 0 \\
&\iff \frac{w_j}{w_i} \geq \frac{s_x^2x_ix_j + s_y^2y_iy_j}{s_x^2x_i^2 + s_y^2y_i^2} = \frac{\mathbf{v}_i \cdot \mathbf{v}_j}{\|\mathbf{v}_i\|^2} = \mathbf{u}_i \cdot \mathbf{u}_j \frac{\|\mathbf{v}_j\|}{\|\mathbf{v}_i\|} \\
&\iff \frac{\omega_j}{\omega_i} \geq \mathbf{u}_i \cdot \mathbf{u}_j
\end{aligned}$$

B The 3-D case

B.1 Error extrema

The coordinates of the points M_a , M_b , and M_c are respectively $M_a = (x_a, y_a, z_a) = (x_iR/\|\mathbf{v}_i\|, y_iR/\|\mathbf{v}_i\|, z_iR/\|\mathbf{v}_i\|)$, $M_b = (x_b, y_b, z_b) = (x_jR/\|\mathbf{v}_j\|, y_jR/\|\mathbf{v}_j\|, z_jR/\|\mathbf{v}_j\|)$, and $M_c = (x_c, y_c, z_c) = (x_kR/\|\mathbf{v}_k\|, y_kR/\|\mathbf{v}_k\|, z_kR/\|\mathbf{v}_k\|)$. We obtain for the error values at these points

$$\begin{aligned}
E(M_a) &= \alpha x_a + \beta y_a + \gamma z_a - R \\
&= \frac{1}{[\mathbf{n}_i, \mathbf{n}_j, \mathbf{n}_k]} \frac{1}{\|\mathbf{v}_i\|} ((x_iy_jz_k - x_iy_kz_j)w_i + (x_iy_kz_i - x_iy_iz_k)w_j + (x_iy_iz_j - x_iy_jz_i)w_k \\
&\quad + (x_ky_iz_j - x_jy_iz_k)w_i + (x_iy_iz_k - x_ky_iz_i)w_j + (x_jy_iz_i - x_iy_iz_j)w_k \\
&\quad + (x_jy_kz_i - x_ky_jz_i)w_i + (x_ky_iz_i - x_iy_kz_i)w_j + (x_iy_jz_i - x_jy_iz_i)w_k) R - R \\
&= \frac{w_i}{\|\mathbf{v}_i\|} R - R
\end{aligned}$$

We obtain similar results for both $E(M_b)$ and $E(M_c)$. Let us examine now $E(M_{ext})$.

$$\begin{aligned}
E(M_{ext}) &= \alpha x_{ext} + \beta y_{ext} + \gamma z_{ext} - R \\
&= \frac{1}{s_x s_y s_z} \sqrt{\alpha^2 s_y^2 s_z^2 + \beta^2 s_x^2 s_z^2 + \gamma^2 s_x^2 s_y^2} R - R
\end{aligned}$$

We have

$$\begin{aligned}
\sqrt{\alpha^2 s_y^2 s_z^2 + \beta^2 s_x^2 s_z^2 + \gamma^2 s_x^2 s_y^2} &= \frac{\|(\mathbf{v}_j \times \mathbf{v}_k)w_i + (\mathbf{v}_k \times \mathbf{v}_i)w_j + (\mathbf{v}_i \times \mathbf{v}_j)w_k\|}{[\mathbf{n}_i, \mathbf{n}_j, \mathbf{n}_k]} \\
&= \|\mathbf{v}_i\| \|\mathbf{v}_j\| \|\mathbf{v}_k\| \frac{\|(\mathbf{u}_j \times \mathbf{u}_k)\omega_i + (\mathbf{u}_k \times \mathbf{u}_i)\omega_j + (\mathbf{u}_i \times \mathbf{u}_j)\omega_k\|}{[\mathbf{n}_i, \mathbf{n}_j, \mathbf{n}_k]}
\end{aligned}$$

Moreover, we have $s_x s_y s_z [\mathbf{n}_i, \mathbf{n}_j, \mathbf{n}_k] = [\mathbf{v}_i, \mathbf{v}_j, \mathbf{v}_k]$, and then $\frac{\|\mathbf{v}_i\| \|\mathbf{v}_j\| \|\mathbf{v}_k\|}{s_x s_y s_z [\mathbf{n}_i, \mathbf{n}_j, \mathbf{n}_k]} = \frac{1}{[\mathbf{u}_i, \mathbf{u}_j, \mathbf{u}_k]}$. From above, it comes

$$\begin{aligned}
E(M_{ext}) &= \frac{1}{s_x s_y s_z} \sqrt{\alpha^2 s_y^2 s_z^2 + \beta^2 s_x^2 s_z^2 + \gamma^2 s_x^2 s_y^2} R - R \\
&= \frac{\|\mathbf{v}_i\| \|\mathbf{v}_j\| \|\mathbf{v}_k\|}{s_x s_y s_z [\mathbf{n}_i, \mathbf{n}_j, \mathbf{n}_k]} \|(\mathbf{u}_j \times \mathbf{u}_k)\omega_i + (\mathbf{u}_k \times \mathbf{u}_i)\omega_j + (\mathbf{u}_i \times \mathbf{u}_j)\omega_k\| R - R \\
&= \frac{\|\omega_i(\mathbf{u}_j \times \mathbf{u}_k) + \omega_j(\mathbf{u}_k \times \mathbf{u}_i) + \omega_k(\mathbf{u}_i \times \mathbf{u}_j)\|}{[\mathbf{u}_i, \mathbf{u}_j, \mathbf{u}_k]} R - R
\end{aligned}$$

B.2 Proof of proposition 5

M_{ext} lies within the sector $(O, \mathbf{u}_i, \mathbf{u}_j, \mathbf{u}_k)$ iff we have $a_{ext} \geq 0$, $b_{ext} \geq 0$, and $c_{ext} \geq 0$, with a_{ext} , b_{ext} , and c_{ext} defined by replacing x , y , and z in the expressions of a , b , and c (Eq. (10)) by x_{ext} , y_{ext} and z_{ext} . We will just detail here the calculations for $a_{ext} \geq 0$, the ones for $b_{ext} \geq 0$ and $c_{ext} \geq 0$ being very similar (they are identical up to a permutations of the indices).

$$a_{ext} \geq 0$$

$$\begin{aligned}
&\iff \frac{1}{[\mathbf{n}_i, \mathbf{n}_j, \mathbf{n}_k]} ((y_j z_k - y_k z_j) x_{ext} + (x_k z_j - x_j z_k) y_{ext} + (x_j y_k - x_k y_j) z_{ext}) \geq 0 \\
&\iff (y_j z_k - y_k z_j) s_y^2 s_z^2 \alpha + (x_k z_j - x_j z_k) s_x^2 s_z^2 \beta + (x_j y_k - x_k y_j) s_x^2 s_y^2 \gamma \geq 0 \\
&\iff \frac{1}{[\mathbf{n}_i, \mathbf{n}_j, \mathbf{n}_k]} (w_i ((y_j z_k - y_k z_j)^2 s_y^2 s_z^2 + (x_k z_j - x_j z_k)^2 s_x^2 s_z^2 + (x_j y_k - x_k y_j)^2 s_x^2 s_y^2) \\
&\quad + w_j ((y_j z_k - y_k z_j)(y_k z_i - y_i z_k) s_y^2 s_z^2 + (x_k z_j - x_j z_k)(x_i z_k - x_k z_i) s_x^2 s_z^2 \\
&\quad + (x_j y_k - x_k y_j)(x_k y_i - x_i y_k) s_x^2 s_y^2) \\
&\quad + w_k ((y_j z_k - y_k z_j)(y_i z_j - y_j z_i) s_y^2 s_z^2 + (x_k z_j - x_j z_k)(x_j z_i - x_i z_j) s_x^2 s_z^2 \\
&\quad + (x_j y_k - x_k y_j)(x_i y_j - x_j y_i) s_x^2 s_y^2)) \geq 0
\end{aligned}$$

The x_p , y_p and z_p are the coordinates of the vectors \mathbf{n}_p . After multiplication by (respectively) s_x , s_y , or s_z , we get $s_x x_p$, $s_y y_p$ and $s_z z_p$ that are the coordinates of the vectors \mathbf{v}_p . For the sake of simplicity of the calculations here, we will from now *omit* the s_x , s_y and s_z , and consider that the x_p , y_p and z_p are the coordinates of the vectors \mathbf{v}_p .

From the above expression, we retrieve the factor of w_i and we get

$$\begin{aligned}
& y_j^2 z_k^2 + y_k^2 z_j^2 - 2y_j y_k z_j z_k + x_k^2 z_j^2 + x_j^2 z_k^2 - 2x_j x_k z_j z_k + x_j^2 y_k^2 + x_k^2 y_j^2 - 2x_j x_k y_j y_k \\
&= \| \mathbf{v}_j \|^2 \| \mathbf{v}_k \|^2 - x_j^2 x_k^2 - y_j^2 y_k^2 - z_j^2 z_k^2 - 2y_j y_k z_j z_k - 2x_j x_k z_j z_k - 2x_j x_k y_j y_k \\
&= \| \mathbf{v}_j \|^2 \| \mathbf{v}_k \|^2 - (\mathbf{v}_j \cdot \mathbf{v}_k)^2 \\
&= \| \mathbf{v}_j \times \mathbf{v}_k \|^2
\end{aligned}$$

After simplification, the factor of w_j becomes

$$\begin{aligned}
& y_j y_k z_i z_k - y_i y_j z_k^2 - y_k^2 z_i z_j + y_i y_k z_j z_k + x_i x_k z_j z_k - x_k^2 z_i z_j - x_i x_j z_k^2 + x_j x_k z_i z_k \\
&+ x_j x_k y_i y_k - x_i x_j y_k^2 - x_k^2 y_i y_j + x_i x_k y_j y_k \\
&= -\| \mathbf{v}_k \|^2 (\mathbf{v}_i \cdot \mathbf{v}_j) + x_i x_j x_k^2 + y_i y_j y_k^2 + z_i z_j z_k^2 \\
&\quad + y_j y_k z_i z_k + y_i y_k z_j z_k + x_i x_k z_j z_k + x_j x_k z_i z_k + x_j x_k y_i y_k + x_i x_k y_j y_k \\
&= (\mathbf{v}_i \cdot \mathbf{v}_k) (\mathbf{v}_j \cdot \mathbf{v}_k) - \| \mathbf{v}_k \|^2 (\mathbf{v}_i \cdot \mathbf{v}_j) \\
&= (\mathbf{v}_k \times \mathbf{v}_i) \cdot (\mathbf{v}_j \times \mathbf{v}_k)
\end{aligned}$$

Similarly, we get for the factor of w_k

$$(\mathbf{v}_i \cdot \mathbf{v}_j) (\mathbf{v}_j \cdot \mathbf{v}_k) - \| \mathbf{v}_j \|^2 (\mathbf{v}_i \cdot \mathbf{v}_k) = (\mathbf{v}_i \times \mathbf{v}_j) \cdot (\mathbf{v}_j \times \mathbf{v}_k)$$

Finally, we have

$$a_{ext} \geq 0$$

$$\iff w_i \| \mathbf{v}_j \times \mathbf{v}_k \|^2 + w_j (\mathbf{v}_k \times \mathbf{v}_i) \cdot (\mathbf{v}_j \times \mathbf{v}_k) + w_k (\mathbf{v}_i \times \mathbf{v}_j) \cdot (\mathbf{v}_j \times \mathbf{v}_k) \geq 0$$

$$\iff (\| \mathbf{v}_i \| \| \mathbf{v}_j \|^2 \| \mathbf{v}_k \|^2) \left(\frac{w_i}{\| \mathbf{v}_i \|} (\mathbf{u}_j \times \mathbf{u}_k) + \frac{w_j}{\| \mathbf{v}_j \|} (\mathbf{u}_k \times \mathbf{u}_i) + \frac{w_k}{\| \mathbf{v}_k \|} (\mathbf{u}_i \times \mathbf{u}_j) \right) \cdot (\mathbf{u}_j \times \mathbf{u}_k) \geq 0$$

B.3 The best possible error in a 3-D sector

Let us examine the scalar product $\mathbf{U}_{ijk} \cdot (\mathbf{u}_j \times \mathbf{u}_k)$. We have

$$\begin{aligned} \mathbf{U}_{ijk} \cdot (\mathbf{u}_j \times \mathbf{u}_k) &= ((\mathbf{u}_j \times \mathbf{u}_k) + (\mathbf{u}_k \times \mathbf{u}_i) + (\mathbf{u}_i \times \mathbf{u}_j)) \cdot (\mathbf{u}_j \times \mathbf{u}_k) \\ &= 1 - (\mathbf{u}_j \cdot \mathbf{u}_k)^2 + (\mathbf{u}_k \cdot \mathbf{u}_j)(\mathbf{u}_i \cdot \mathbf{u}_k) - (\mathbf{u}_i \cdot \mathbf{u}_j) + (\mathbf{u}_i \cdot \mathbf{u}_j)(\mathbf{u}_j \cdot \mathbf{u}_k) - (\mathbf{u}_i \cdot \mathbf{u}_k) \\ &= (1 - (\mathbf{u}_j \cdot \mathbf{u}_k))(1 + (\mathbf{u}_j \cdot \mathbf{u}_k) - (\mathbf{u}_i \cdot \mathbf{u}_j) - (\mathbf{u}_k \cdot \mathbf{u}_i)) \end{aligned}$$

Hence (recall that the \mathbf{u}_n are unit vectors)

$$\begin{aligned} \mathbf{U}_{ijk} \cdot (\mathbf{u}_j \times \mathbf{u}_k) < 0 &\iff 1 + (\mathbf{u}_j \cdot \mathbf{u}_k) - (\mathbf{u}_i \cdot \mathbf{u}_j) - (\mathbf{u}_k \cdot \mathbf{u}_i) < 0 \\ &\iff (\mathbf{u}_j \cdot \mathbf{u}_k) < (\mathbf{u}_i \cdot \mathbf{u}_j) + (\mathbf{u}_k \cdot \mathbf{u}_i) - 1 \\ &\implies \begin{cases} (\mathbf{u}_j \cdot \mathbf{u}_k) < (\mathbf{u}_i \cdot \mathbf{u}_j) \\ (\mathbf{u}_j \cdot \mathbf{u}_k) < (\mathbf{u}_k \cdot \mathbf{u}_i) \end{cases} \end{aligned}$$

On the other hand, we have

$$\begin{aligned} H_{jk} < H_{ij} &\iff \|\mathbf{u}_j + \mathbf{u}_k\|^2 < \|\mathbf{u}_i + \mathbf{u}_j\|^2 \\ &\iff (\mathbf{u}_j + \mathbf{u}_k) \cdot (\mathbf{u}_j + \mathbf{u}_k) < (\mathbf{u}_i + \mathbf{u}_j) \cdot (\mathbf{u}_i + \mathbf{u}_j) \\ &\iff (\mathbf{u}_j \cdot \mathbf{u}_k) < (\mathbf{u}_i \cdot \mathbf{u}_j) \end{aligned}$$

It comes then

$$\mathbf{U}_{ijk} \cdot (\mathbf{u}_j \times \mathbf{u}_k) < 0 \implies \begin{cases} H_{jk} < H_{ij} \\ H_{jk} < H_{ki} \end{cases}$$

B.4 Convexity criterium: proof of proposition 9

Let us examine

$$\begin{aligned} &\omega_j \left([\mathbf{u}_i, \mathbf{u}_k, \mathbf{u}_l](\mathbf{u}_j \times \mathbf{u}_k) - [\mathbf{u}_j, \mathbf{u}_l, \mathbf{u}_k](\mathbf{u}_k \times \mathbf{u}_i) - [\mathbf{u}_i, \mathbf{u}_j, \mathbf{u}_k](\mathbf{u}_k \times \mathbf{u}_l) \right) \cdot (\mathbf{u}_j \times \mathbf{u}_k) \\ &- \omega_k \left([\mathbf{u}_i, \mathbf{u}_j, \mathbf{u}_l](\mathbf{u}_j \times \mathbf{u}_k) + [\mathbf{u}_j, \mathbf{u}_l, \mathbf{u}_k](\mathbf{u}_i \times \mathbf{u}_j) + [\mathbf{u}_i, \mathbf{u}_j, \mathbf{u}_k](\mathbf{u}_l \times \mathbf{u}_j) \right) \cdot (\mathbf{u}_j \times \mathbf{u}_k) \end{aligned}$$

It can be noticed that the factor of ω_k is identical to the one of ω_j , up to a permutation of the indices j and k , so we will just examine the vector

$$[\mathbf{u}_i, \mathbf{u}_k, \mathbf{u}_l](\mathbf{u}_j \times \mathbf{u}_k) - [\mathbf{u}_j, \mathbf{u}_l, \mathbf{u}_k](\mathbf{u}_k \times \mathbf{u}_i) - [\mathbf{u}_i, \mathbf{u}_j, \mathbf{u}_k](\mathbf{u}_k \times \mathbf{u}_l)$$

Each of its coordinates can be calculated as follows (with (A, B) denoting one of the couples (y, z) , (z, x) , or (x, y))

$$\begin{aligned} &(x_i y_k z_l + x_l y_i z_k + x_k y_l z_i - x_i y_l z_k - x_k y_i z_l - x_l y_k z_i)(A_j B_k - A_k B_j) \\ &+ (x_j y_l z_k + x_k y_j z_l + x_l y_k z_j - x_j y_k z_l - x_l y_j z_k - x_k y_l z_j)(A_i B_k - A_k B_i) \\ &+ (x_i y_j z_k + x_k y_i z_j + x_j y_k z_i - x_i y_k z_j - x_j y_i z_k - x_k y_j z_i)(A_l B_k - A_k B_l) \end{aligned}$$

$$\begin{aligned}
= & x_k A_k (-y_l z_i B_j + y_i z_l B_j - y_j z_l B_i + y_l z_j B_i - y_i z_j B_l + y_j z_i B_l) \\
& + x_k B_k (y_l z_i A_j - y_i z_l A_j + y_j z_l A_i - y_l z_j A_i + y_i z_j A_l - y_j z_i A_l) \\
& + y_k A_k (-x_i z_l B_j + x_l z_i B_j - x_l z_j B_i + x_j z_l B_i - x_j z_i B_l + x_i z_j B_l) \\
& + y_k B_k (x_i z_l A_j - x_l z_i A_j + x_l z_j A_i - x_j z_l A_i + x_j z_i A_l - x_i z_j A_l) \\
& + z_k A_k (-x_l y_i B_j + x_i y_l B_j - x_j y_l B_i + x_l y_j B_i - x_i y_j B_l + x_j y_i B_l) \\
& + z_k B_k (x_l y_i A_j - x_i y_l A_j + x_j y_l A_i - x_l y_j A_i + x_i y_j A_l - x_j y_i A_l)
\end{aligned}$$

It can be remarked that

- the factor of $x_k A_k$ becomes zero for $B \in \{y, z\}$,
- the factor of $x_k B_k$ becomes zero for $A \in \{y, z\}$,
- the factor of $y_k A_k$ becomes zero for $B \in \{x, z\}$,
- the factor of $y_k B_k$ becomes zero for $A \in \{x, z\}$,
- the factor of $z_k A_k$ becomes zero for $B \in \{x, y\}$,
- the factor of $z_k B_k$ becomes zero for $A \in \{x, y\}$.

For (A, B) denoting respectively (y, z) , (z, x) , and (x, y) , we have still the factors of respectively $y_k B_k = y_k z_k$ and $z_k A_k = z_k y_k$, $x_k A_k = x_k z_k$ and $z_k B_k = z_k x_k$, and $x_k B_k = x_k y_k$ and $y_k A_k = y_k x_k$ to evaluate. In each of these cases, we can factorize respectively $y_k z_k$, $x_k z_k$ or $x_k y_k$, and it can be verified that the sum of the two factors is zero.

Thus we have

$$[\mathbf{u}_i, \mathbf{u}_k, \mathbf{u}_l](\mathbf{u}_j \times \mathbf{u}_k) - [\mathbf{u}_j, \mathbf{u}_l, \mathbf{u}_k](\mathbf{u}_k \times \mathbf{u}_i) - [\mathbf{u}_i, \mathbf{u}_j, \mathbf{u}_k](\mathbf{u}_k \times \mathbf{u}_l) = \mathbf{0}$$



Unité de recherche INRIA Sophia Antipolis
2004, route des Lucioles - BP 93 - 06902 Sophia Antipolis Cedex (France)

Unité de recherche INRIA Futurs : Parc Club Orsay Université - ZAC des Vignes
4, rue Jacques Monod - 91893 ORSAY Cedex (France)

Unité de recherche INRIA Lorraine : LORIA, Technopôle de Nancy-Brabois - Campus scientifique
615, rue du Jardin Botanique - BP 101 - 54602 Villers-lès-Nancy Cedex (France)

Unité de recherche INRIA Rennes : IRISA, Campus universitaire de Beaulieu - 35042 Rennes Cedex (France)

Unité de recherche INRIA Rhône-Alpes : 655, avenue de l'Europe - 38334 Montbonnot Saint-Ismier (France)

Unité de recherche INRIA Rocquencourt : Domaine de Voluceau - Rocquencourt - BP 105 - 78153 Le Chesnay Cedex (France)

Éditeur
INRIA - Domaine de Voluceau - Rocquencourt, BP 105 - 78153 Le Chesnay Cedex (France)
<http://www.inria.fr>
ISSN 0249-6399